

**Figure 2.** VEGFR-1 deletion induces activation of the p53/p21 signal pathway. **A**, A luciferase reporter gene plasmid (pPG13-Luc) containing the p53-binding sequence was transfected into endothelial cells infected with shNega, shVEGFR-1, or shVEGFR-2. Luciferase activity was measured at 48 hours after transfection in the presence of VEGF-A (10 ng/mL) as described in Methods. \* $P < 0.05$  vs shNega ( $n = 5$ ). **B**, Whole cell lysates (30  $\mu$ g) were prepared from infected endothelial cells and p21 expression was assessed by Western blot analysis. \* $P < 0.05$  vs shNega, # $P < 0.01$  vs shVEGFR-2 ( $n = 4$ ). **C**, Human endothelial cells were infected with pLNCX (Mock) or pLNCX E6 (E6). Infected cell populations were then transduced with shNega or shVEGFR-1. After purification, double-infected cells were seeded at a density of  $2 \times 10^5$  cells per 100-mm dish in the presence of VEGF-A (day 0), and cell number was counted on day 3. \* $P < 0.05$  vs Mock/shNega ( $n = 3$ ). Western blot analysis revealed that introduction of E6 effectively ablated p53 expression (right panel).

### Influence of VEGFR-1 Deletion on Neovascularization In Vivo

To examine the influence of VEGFR-1 deletion on neovascularization in vivo, we produced a hindlimb ischemia model in VEGFR-1<sup>+/-</sup> mice and assessed blood flow recovery and the capillary density of ischemic tissue. VEGFR-1 mRNA levels were significantly lower in VEGFR-1<sup>+/-</sup> mice than in wild-type mice (Figure 4A). Aortic expression of VEGFR-1 protein was decreased in VEGFR-1<sup>+/-</sup> mice compared with wild-type mice (Figure 4B). Consistent with the in vitro data, phospho-Akt levels were significantly higher in VEGFR-1<sup>+/-</sup> mice than in wild-type mice (Figure 4C and supplemental Figure III). There was no significant difference in plasma VEGF levels between the two groups (data not shown). Laser Doppler image analysis revealed that blood flow recovery

was significantly impaired in VEGFR-1<sup>+/-</sup> mice compared with their wild-type littermates (Figure 4D). Likewise, VEGFR-1<sup>+/-</sup> mice exhibited significantly fewer CD31-positive cells in the ischemic tissues than their wild-type littermates (Figure 4E), suggesting that decreased expression of VEGFR-1 led to reduced neovascularization of ischemic tissue.

There are several reports indicating that VEGFR-1 kinase activity is required for VEGF-induced migration of hematopoietic cells including macrophages,<sup>21–26</sup> and it was reported that infiltration of macrophages plays a critical role in pathological angiogenesis during ischemia, inflammation, and tumor development.<sup>27–29</sup> Therefore, we examined the number of infiltrating macrophages in ischemic tissue, but we found no significant difference in the number of Mac3-

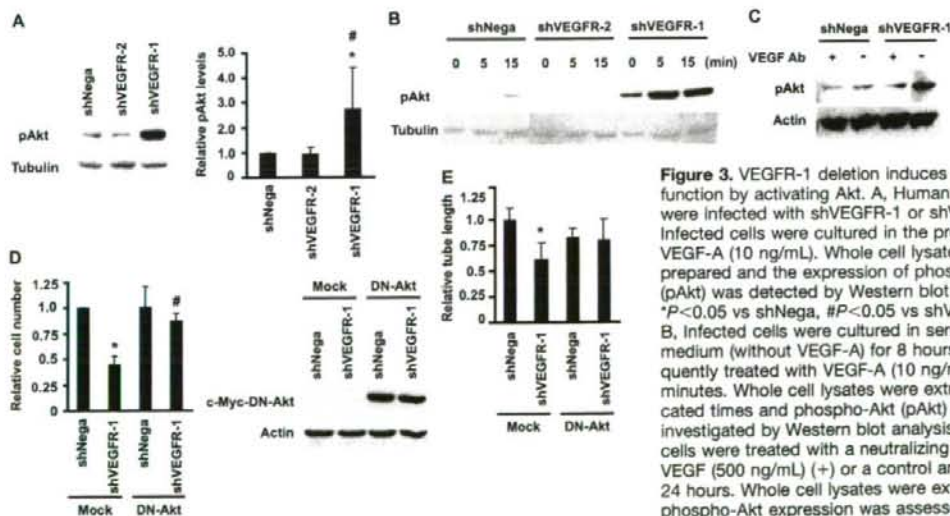


**Figure 3.** VEGFR-1 deletion induces endothelial dysfunction by activating Akt. **A**, Human endothelial cells were infected with shVEGFR-1 or shVEGFR-2. Infected cells were cultured in the presence of VEGF-A (10 ng/mL). Whole cell lysates (30  $\mu$ g) were prepared and the expression of phosphorylated Akt (pAkt) was detected by Western blot analysis. \* $P < 0.05$  vs shNega, # $P < 0.05$  vs shVEGFR-2 ( $n = 5$ ). **B**, Infected cells were cultured in serum-free basal medium (without VEGF-A) for 8 hours and subsequently treated with VEGF-A (10 ng/mL) for 5 to 15 minutes. Whole cell lysates were extracted at indicated times and phospho-Akt (pAkt) expression was investigated by Western blot analysis. **C**, Infected cells were treated with a neutralizing antibody for VEGF (500 ng/mL) (+) or a control antibody (-) for 24 hours. Whole cell lysates were extracted and phospho-Akt expression was assessed by Western blot analysis. **D**, Human endothelial cells were infected with pLNCX (Mock) or pLNCX DN-Akt (DN-Akt). Infected cell populations were then transduced with shNega or shVEGFR-1 and were subjected to the proliferation assay as described in legend for Figure 2C. \* $P < 0.005$  vs Mock/shNega, # $P < 0.005$  vs Mock/shVEGFR-1 ( $n = 6$  to 8). Expression of c-Myc-tagged DN-Akt was confirmed by Western blot analysis (right panel). **E**, Double-infected endothelial cells (prepared as in Figure 3C) were subjected to the tube-forming assay. \* $P < 0.05$  vs Mock/shNega ( $n = 3$ ).

infected with pLNCX (Mock) or pLNCX DN-Akt (DN-Akt). Infected cell populations were then transduced with shNega or shVEGFR-1 and were subjected to the proliferation assay as described in legend for Figure 2C. \* $P < 0.005$  vs Mock/shNega, # $P < 0.005$  vs Mock/shVEGFR-1 ( $n = 6$  to 8). Expression of c-Myc-tagged DN-Akt was confirmed by Western blot analysis (right panel). **E**, Double-infected endothelial cells (prepared as in Figure 3C) were subjected to the tube-forming assay. \* $P < 0.05$  vs Mock/shNega ( $n = 3$ ).

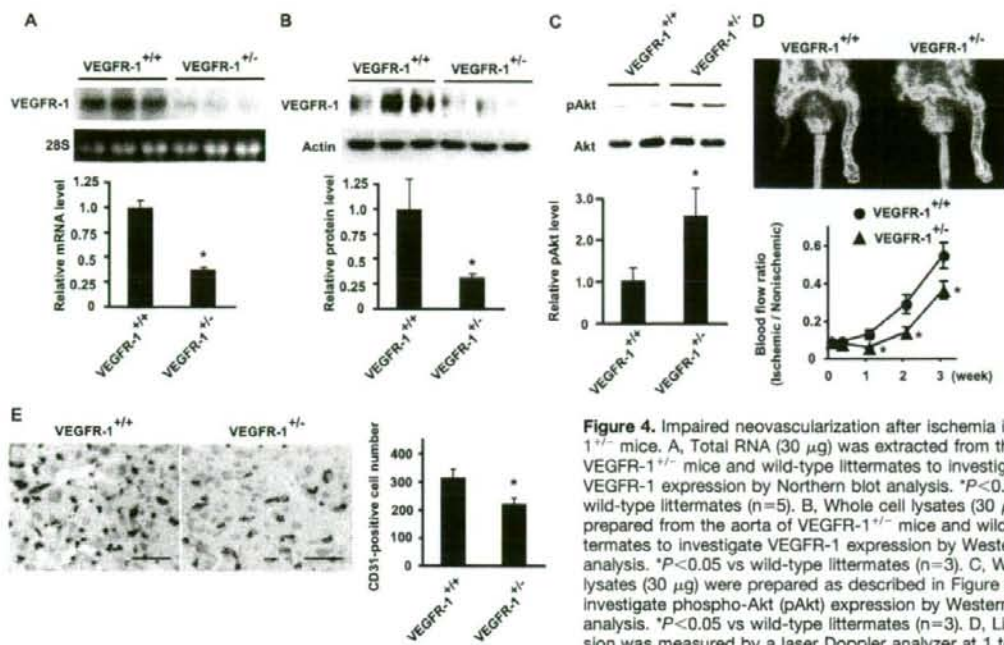


**Figure 4.** Impaired neovascularization after ischemia in VEGFR-1<sup>-/-</sup> mice. **A**, Total RNA (30  $\mu$ g) was extracted from the lung of VEGFR-1<sup>-/-</sup> mice and wild-type littermates to investigate VEGFR-1 expression by Northern blot analysis. \* $P < 0.001$  vs wild-type littermates ( $n = 5$ ). **B**, Whole cell lysates (30  $\mu$ g) were prepared from the aorta of VEGFR-1<sup>-/-</sup> mice and wild-type littermates to investigate VEGFR-1 expression by Western blot analysis. \* $P < 0.05$  vs wild-type littermates ( $n = 3$ ). **C**, Whole cell lysates (30  $\mu$ g) were prepared as described in Figure 4B to investigate phospho-Akt (pAkt) expression by Western blot analysis. \* $P < 0.05$  vs wild-type littermates ( $n = 3$ ). **D**, Limb perfusion was measured by a laser Doppler analyzer at 1 to 3 weeks after ischemia. The graph shows the ratio of ischemic (right) to nonischemic limb (left) blood flow. \* $P < 0.05$  vs wild-type littermates ( $n = 16$ ). **E**, Immunohistochemistry for CD31 (brown) in ischemic limbs. Scale bar: 50  $\mu$ m. The number of CD31-positive cells per square millimeter is shown in the graph. \* $P < 0.05$  vs wild-type littermates ( $n = 4$ ).

nonischemic limb (left) blood flow. \* $P < 0.05$  vs wild-type littermates ( $n = 16$ ). **E**, Immunohistochemistry for CD31 (brown) in ischemic limbs. Scale bar: 50  $\mu$ m. The number of CD31-positive cells per square millimeter is shown in the graph. \* $P < 0.05$  vs wild-type littermates ( $n = 4$ ).

positive cells between VEGFR-1<sup>-/-</sup> mice and their wild-type littermates (Figure 5A). To further test the possible involvement of bone marrow-derived cells, we transplanted wild-type bone marrow cells into VEGFR-1<sup>-/-</sup> mice or their wild-type littermates. We then produced a hindlimb ischemia model and assessed blood flow recovery and the capillary density of ischemic tissue. Despite the transplantation of wild-type bone marrow, blood flow recovery was still significantly impaired in VEGFR-1<sup>-/-</sup> mice (Figure 5B). The number of CD31-positive cells was also lower in VEGFR-1<sup>-/-</sup> mice than in their wild-type littermates (Figure 5C). Thus, it is unlikely that impaired neovascularization in VEGFR-1<sup>-/-</sup> mice is attributed to reduced migration of bone marrow-derived cells. We could not detect VEGFR-1 expression in muscle cells (supplemental Figure IV). It was noted that the number of endothelial cells double positive for phospho-Akt and CD31 was significantly higher in VEGFR-1<sup>-/-</sup> mice than in their wild-type littermates (Figure 5D).

### Inhibition of Akt Signaling Ameliorates the Impairment of Neovascularization in VEGFR-1<sup>-/-</sup> Mice

Next, we examined whether an increase of endothelial Akt activity contributed to impaired neovascularization in VEGFR-1<sup>-/-</sup> mice. Akt1 is the predominant isoform of Akt in endothelial cells and is thought to play an important role in postnatal angiogenesis.<sup>30</sup> It has been reported that the angiogenic response of Akt1<sup>-/-</sup> mice was enhanced in a tumor angiogenesis model, but was decreased in a hindlimb ischemia

model,<sup>30,31</sup> so we thus used Akt1<sup>-/-</sup> mice for our *in vivo* experiments. Consistent with the previous reports,<sup>32</sup> phospho-Akt levels were lower in the aorta of Akt1<sup>-/-</sup> mice compared with wild-type littermates (supplemental Figure V). After creating hindlimb ischemia in VEGFR-1<sup>-/-</sup> Akt1<sup>-/-</sup> mice, we examined the extent of blood flow recovery and the capillary density 1 week later. We found that there were no significant differences of blood flow recovery and capillary density between Akt1<sup>-/-</sup> mice and Akt1<sup>+/+</sup> mice (Figure 6A and 6B). Decreased VEGFR-1 expression significantly reduced blood flow recovery in Akt1<sup>+/+</sup> mice, but not in Akt1<sup>-/-</sup> mice (Figure 6A). Likewise, the capillary density of ischemic tissue was significantly reduced in VEGFR-1<sup>-/-</sup> Akt1<sup>+/+</sup> mice compared with wild-type mice, but VEGFR-1<sup>-/-</sup> Akt1<sup>-/-</sup> mice had a similar capillary density to that of VEGFR-1<sup>+/+</sup> Akt1<sup>-/-</sup> mice (Figure 6B). These results suggest that an increase of endothelial Akt activity may be responsible for impaired neovascularization in VEGFR-1<sup>-/-</sup> mice.

### Discussion

In the present study, we demonstrated that VEGFR-1 modulates postnatal angiogenesis through inhibition of the excessive activation of Akt by VEGF. It has been reported that VEGF and VEGFR-1 can be simultaneously induced by various stimuli, including hypoxia.<sup>33</sup> Thus, the role of VEGFR-1 may vary, depending on the extent of activation of Akt. For example, when overproduction of growth factors such as VEGF and insulin leads to excessive activation of Akt and impairs normal regulation of endothelial proliferation,



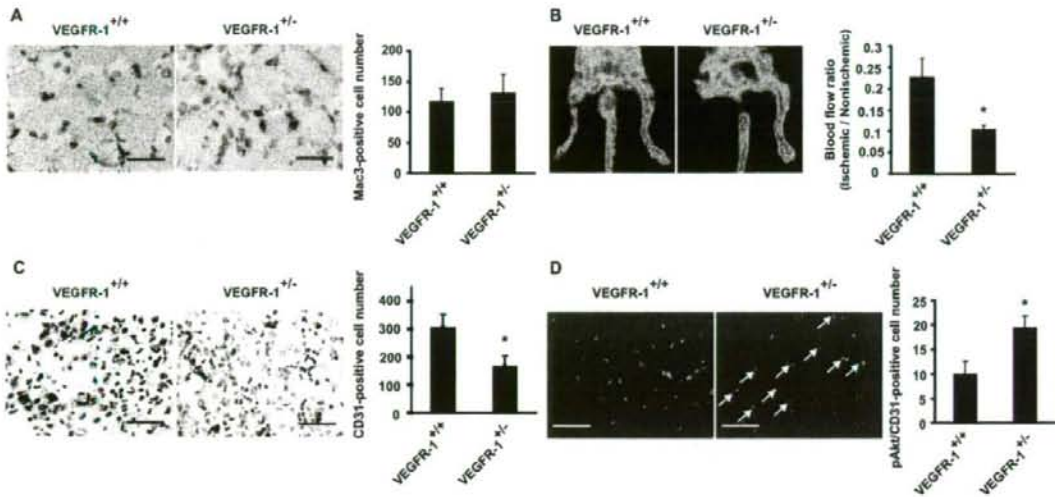


**Figure 5.** Role of bone marrow–derived cells in impaired neovascularization in VEGFR-1<sup>-/-</sup> mice. **A**, Immunohistochemistry for Mac3 (brown) in ischemic limbs. Scale bar: 50  $\mu$ m. The number of Mac3-positive cells per square millimeter is shown (n=4). **B**, Wild-type bone marrow cells were transplanted into VEGFR-1<sup>-/-</sup> mice or their wild-type littermates (n=6). Limb perfusion was measured by a laser Doppler analyzer at 1 week after ischemia. \**P*<0.05 vs wild-type littermates (n=6). **C**, Immunohistochemistry for CD31 (brown) in ischemic limbs of bone marrow–transplanted mice. Scale bar: 50  $\mu$ m. \**P*<0.05 vs wild-type littermates (n=6). **D**, Activation of Akt in endothelial cells of ischemic limbs from VEGFR-1<sup>-/-</sup> mice. Representative immunostainings for phospho-Akt (red) and CD31 (green) were shown. Arrows indicate phospho-Akt/CD31-positive cells (yellow). Scale bar: 50  $\mu$ m. The graph shows the ratio of phospho-Akt/CD31-positive cell number to all CD31-positive cell number. \**P*<0.05 vs wild-type littermates (n=5).

VEGFR-1 may act as a positive regulator of angiogenesis by inhibiting activation of VEGFR-2. Conversely, VEGFR-1 may exert a negative effect on angiogenesis when growth factors appropriately activate the Akt signaling pathway to induce endothelial cell proliferation. These mechanisms may provide an explanation as to why the effects of PIGF on angiogenesis were reported to differ.

Although there is evidence to suggest that VEGFR-1 interacts with the p85 subunit of phosphatidylinositol-3 ki-

nase (PI3K) to regulate its activity,<sup>34–36</sup> VEGFR-1 appears to exert its inhibitory effect on angiogenesis mainly by blocking the activation of Akt mediated by VEGF via VEGFR-2 for the following reasons. First, treatment with VEGF-A increased Akt activity in VEGFR-1–deleted cells, but not in VEGFR-2–deleted cells (Figure 3A and 3B). Second, treatment with a neutralizing anti-VEGF antibody reduced the enhanced activation of Akt in VEGFR-1–deleted cells (Figure 3C). Finally, treatment with PIGF did not provoke any

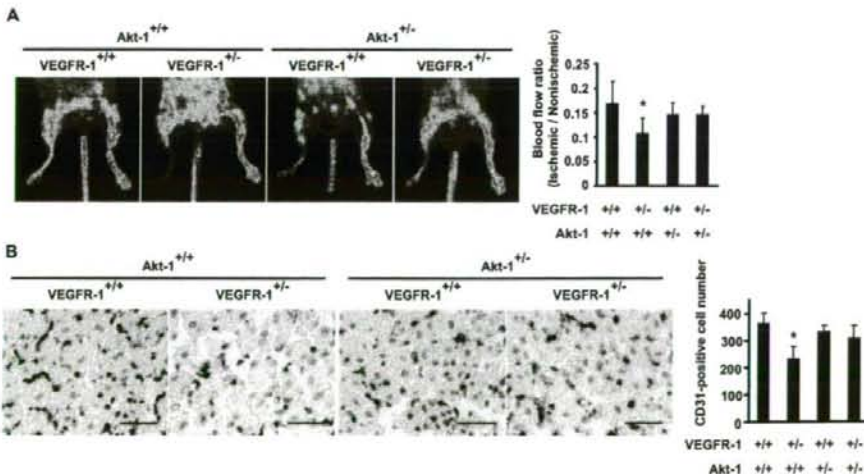


**Figure 6.** Inhibition of Akt signaling ameliorates the impairment of neovascularization in VEGFR-1<sup>-/-</sup> mice. **A**, Limb perfusion was measured by a laser Doppler analyzer at 1 week after creation of ischemia. \**P*<0.01 vs wild-type littermates (n=14 to 18). **B**, Immunohistochemistry for CD31 (brown) in ischemic limbs. Scale bar: 50  $\mu$ m. \**P*<0.05 vs wild-type littermates (n=6 to 7).

biological response in the presence of anti-VEGF antibody (J. Nishi, T. Minamino, unpublished data, 2007). Our results are consistent with previous studies<sup>37,38</sup> demonstrating that tyrosine phosphorylation of VEGFR-2 was elevated in VEGFR-1-deficient embryonic stem cells, whereas loss of VEGFR-1 led to decreased sprout formation and migration, which resulted in reduced vascular branching. This reduction was restored by blockade of the VEGFR-2 signaling pathway as well as by treatment with soluble VEGFR-1. Although Bussolati et al demonstrated that VEGFR-1 but not VEGFR-2 increases endothelial production of NO, thereby promoting tube formation,<sup>39</sup> cGMP production was significantly decreased in VEGFR-1-deleted endothelial cells (supplemental Figure ID). Moreover, VEGF treatment failed to activate Akt in VEGFR-2-deleted endothelial cells (Figure 3B) and introduction of mutant VEGFR-1 lacking the sites for interaction with PI3K did not mimic the effects of shVEGFR-1 (J. Nishi, T. Minamino, unpublished data, 2007). Taken together, these results suggest that VEGFR-1 acts to provide "fine tuning" of VEGF signaling to achieve the proper formation of blood vessels. The biological consequences of VEGFR-1 deletion appears to be related to loss of its decoy effect, but other mechanisms might be involved such as "cross talk" between VEGFR-1 and VEGFR-2,<sup>8,16,17</sup> direct regulation of the VEGFR-2 signaling pathway by VEGFR-1,<sup>39,40</sup> and some undefined effect of the extracellular domain of membrane-bound VEGFR-1.<sup>41</sup>

We have previously demonstrated that constitutive activation of Akt induced by insulin promotes senescence-like arrest of endothelial cell growth via a p53/p21-dependent pathway.<sup>19</sup> Moreover, tube formation was significantly reduced by overactivation of Akt. Likewise, constitutive activation of Akt has been reported to promote the senescence in other types of cells such as endothelial progenitors and mouse embryonic fibroblasts.<sup>42,43</sup> The study using conditional transgenic mice has demonstrated that sustained activation of Akt in endothelial cells causes increased blood vessel size and generalized edema within 2 weeks and that these changes are reversible.<sup>44</sup> Using the same mouse model, it has been reported that chronic activation of Akt over 8 weeks leads to endothelial cell senescence and loss of endothelium-dependent stroke protection.<sup>45</sup> Recent studies by several groups demonstrated that diabetic state induces activation of the Akt pathway, thereby contributing to the pathology of diabetic complications.<sup>42,46–48</sup> We also detected increased Akt activity in endothelial cells on the surface of coronary atherosclerotic lesions in patients with diabetes.<sup>19</sup> Moreover, accumulating evidence suggests that vascular cell senescence contributes to the pathogenesis of age-associated vascular diseases including diabetic vasculopathy.<sup>49</sup> Thus, these results suggest the potential of the treatment for vascular dysfunction associated with diabetes and aging by modulating Akt activity with a soluble form of VEGFR-1.

### Acknowledgments

We thank Dr B. Vogelstein and Dr T. Zioncheck for reagents, Dr M. Birnbaum for mice, and E. Fujita, Y. Ishiyama, R. Kobayashi, and Y. Ishikawa for their excellent technical assistance.

### Sources of Funding

This work was supported by a Grant-in-Aid for Scientific Research from the Ministry of Education, Science, Sports, and Culture, and Health and Labor Sciences Research Grants (to I.K.) and a Grant-in-Aid for Scientific Research from the Ministry of Education, Culture, Sports, Science, and Technology of Japan, and the grants from the Suzuki Memorial Foundation, the Japan Diabetes Foundation, the Ichiro Kanehara Foundation, the Tokyo Biochemical Research Foundation, the Takeda Science Foundation, the Cell Science Research Foundation, and the Japan Foundation of Applied Enzymology (to T.M.).

### Disclosures

None.

### References

- Carmeliet P. Angiogenesis in life, disease and medicine. *Nature*. 2005; 438:932–936.
- Ferrara N, Gerber HP, LeCouter J. The biology of VEGF and its receptors. *Nat Med*. 2003;9:669–676.
- Coulas L, Chawengsaksophak K, Rossant J. Endothelial cells and VEGF in vascular development. *Nature*. 2005;438:937–945.
- Fong GH, Rossant J, Gertsenstein M, Breitman ML. Role of the Flt-1 receptor tyrosine kinase in regulating the assembly of vascular endothelium. *Nature*. 1995;376:66–70.
- Fong GH, Zhang L, Bryce DM, Peng J. Increased hemangioblast commitment, not vascular disorganization, is the primary defect in flt-1 knock-out mice. *Development*. 1999;126:3015–3025.
- Kearney JB, Ambler CA, Monaco KA, Johnson N, Rapoport RG, Baugh VL. Vascular endothelial growth factor receptor Flt-1 negatively regulates developmental blood vessel formation by modulating endothelial cell division. *Blood*. 2002;99:2397–2407.
- Hiratsuka S, Minowa O, Kuno J, Noda T, Shibuya M. Flt-1 lacking the tyrosine kinase domain is sufficient for normal development and angiogenesis in mice. *Proc Natl Acad Sci U S A*. 1998;95:9349–9354.
- Rahimi N, Dayanir V, Lashkari K. Receptor chimeras indicate that the vascular endothelial growth factor receptor-1 (VEGFR-1) modulates mitogenic activity of VEGFR-2 in endothelial cells. *J Biol Chem*. 2000;275: 16986–16992.
- Keyt BA, Nguyen HV, Berleau LT, Duarte CM, Park J, Chen H, Ferrara N. Identification of vascular endothelial growth factor determinants for binding KDR and FLT-1 receptors. Generation of receptor-selective VEGF variants by site-directed mutagenesis. *J Biol Chem*. 1996;271: 5638–5646.
- Yang S, Xin X, Zlot C, Ingle G, Fuh G, Li B, Moffat B, de Vos AM, Gerritsen ME. Vascular endothelial cell growth factor-driven endothelial tube formation is mediated by vascular endothelial cell growth factor receptor-2, a kinase insert domain-containing receptor. *Arterioscler Thromb Vasc Biol*. 2001;21:1934–1940.
- Gille H, Kowalski J, Li B, LeCouter J, Moffat B, Zioncheck TF, Pelletier N, Ferrara N. Analysis of biological effects and signaling properties of Flt-1 (VEGFR-1) and KDR (VEGFR-2). A reassessment using novel receptor-specific vascular endothelial growth factor mutants. *J Biol Chem*. 2001;276:3222–3230.
- Errico M, Riccioni T, Iyer S, Pisano C, Acharya KR, Persico MG, De Falco S. Identification of placenta growth factor determinants for binding and activation of Flt-1 receptor. *J Biol Chem*. 2004;279:43929–43939.
- Luttun A, Tjwa M, Moons L, Wu Y, Angelillo-Scherer A, Liao F, Nagy JA, Hooper A, Priller J, De Klerck B, Compernelle V, Daci E, Bohlen P, Dewerchin M, Herbert JM, Fava R, Matthys P, Carmeliet G, Collen D, Dvorak HF, Hicklin DJ, Carmeliet P. Revascularization of ischemic tissues by PIGF treatment, and inhibition of tumor angiogenesis, arthritis and atherosclerosis by anti-Flt1. *Nat Med*. 2002;8:831–840.
- Adini A, Kornaga T, Firoozbakhsh F, Benjamin LE. Placental growth factor is a survival factor for tumor endothelial cells and macrophages. *Cancer Res*. 2002;62:2749–2752.
- Odoriso T, Schietroma C, Zaccaria ML, Cianfarani F, Tiverton C, Tatangelo L, Failla CM, Zambruno G. Mice overexpressing placenta growth factor exhibit increased vascularization and vessel permeability. *J Cell Sci*. 2002;115:2559–2567.
- Autiero M, Waltenberger J, Communi D, Kranz A, Moons L, Lambrechts D, Kroll J, Plaisance S, De Mol M, Bono F, Kliche S, Fellbrich G, Ballmer-Hofer K, Maglione D, Mayr-Beyle U, Dewerchin M, Dom-



- browski S, Stanimirovic D, Van Hummelen P, Dehio C, Hicklin DJ, Persico G, Herbert JM, Communi D, Shibuya M, Collen D, Conway EM, Carmeliet P. Role of PlGF in the intra- and intermolecular cross talk between the VEGF receptors Flt1 and Flk1. *Nat Med*. 2003;9:936-943.
17. Neaogoe PE, Lemieux C, Sirois MG. Vascular endothelial growth factor (VEGF)-A165-induced prostacyclin synthesis requires the activation of VEGF receptor-1 and -2 heterodimer. *J Biol Chem*. 2005;280:9904-9912.
  18. Shih SC, Ju M, Liu N, Smith LE. Selective stimulation of VEGFR-1 prevents oxygen-induced retinal vascular degeneration in retinopathy of prematurity. *J Clin Invest*. 2003;112:50-57.
  19. Miyauchi H, Minamino T, Tateo K, Kunieda T, Toko H, Komuro I. Akt negatively regulates the in vitro lifespan of human endothelial cells via a p53/p21-dependent pathway. *Embo J*. 2004;23:212-220.
  20. O'Neill BT, Abel ED. Akt1 in the cardiovascular system: friend or foe? *J Clin Invest*. 2005;115:2059-2064.
  21. Clauss M, Weich H, Breier G, Knies U, Rockl W, Waltenberger J, Risau W. The vascular endothelial growth factor receptor Flt-1 mediates biological activities. Implications for a functional role of placenta growth factor in monocyte activation and chemotaxis. *J Biol Chem*. 1996;271:17629-17634.
  22. Barleon B, Sozzani S, Zhou D, Weich HA, Mantovani A, Marme D. Migration of human monocytes in response to vascular endothelial growth factor (VEGF) is mediated via the VEGF receptor flt-1. *Blood*. 1996;87:3336-3343.
  23. Sawano A, Iwai S, Sakurai Y, Ito M, Shitara K, Nakahata T, Shibuya M. Flt-1, vascular endothelial growth factor receptor 1, is a novel cell surface marker for the lineage of monocyte-macrophages in humans. *Blood*. 2001;97:785-791.
  24. Lyden D, Hattori K, Dias S, Costa C, Blaikie P, Butros L, Chadburn A, Heissig B, Marks W, Witte L, Wu Y, Hicklin D, Zhu Z, Hackett NR, Crystal RG, Moore MA, Hajar KA, Manova K, Benezra R, Rafii S. Impaired recruitment of bone-marrow-derived endothelial and hematopoietic precursor cells blocks tumor angiogenesis and growth. *Nat Med*. 2001;7:1194-1201.
  25. Hattori K, Heissig B, Wu Y, Dias S, Tejada R, Ferris B, Hicklin DJ, Zhu Z, Bohlen P, Witte L, Hendrikx J, Hackett NR, Crystal RG, Moore MA, Werb Z, Lyden D, Rafii S. Placental growth factor reconstitutes hematopoiesis by recruiting VEGFR1(+) stem cells from bone-marrow microenvironment. *Nat Med*. 2002;8:841-849.
  26. Jin DK, Shido K, Kopp HG, Petit I, Shmelkov SV, Young LM, Hooper AT, Amano H, Avezilla ST, Heissig B, Hattori K, Zhang F, Hicklin DJ, Wu Y, Zhu Z, Dunn A, Salari H, Werb Z, Hackett NR, Crystal RG, Lyden D, Rafii S. Cytokine-mediated deployment of SDF-1 induces revascularization through recruitment of CXCR4+ hemangiocytes. *Nat Med*. 2006;12:557-567.
  27. Carmeliet P. Mechanisms of angiogenesis and arteriogenesis. *Nat Med*. 2000;6:389-395.
  28. Hiratsuka S, Maru Y, Okada A, Seiki M, Noda T, Shibuya M. Involvement of Flt-1 tyrosine kinase (vascular endothelial growth factor receptor-1) in pathological angiogenesis. *Cancer Res*. 2001;61:1207-1213.
  29. Murakami M, Iwai S, Hiratsuka S, Yamauchi M, Nakamura K, Iwakura Y, Shibuya M. Signaling of vascular endothelial growth factor receptor-1 tyrosine kinase promotes rheumatoid arthritis through activation of monocytes/macrophages. *Blood*. 2006;108:1849-1856.
  30. Chen J, Somanath PR, Razorenova O, Chen WS, Hay N, Bornstein P, Byzova TV. Akt1 regulates pathological angiogenesis, vascular maturation and permeability in vivo. *Nat Med*. 2005;11:1188-1196.
  31. Ackah E, Yu J, Zoellner S, Iwakiri Y, Skurc C, Shibata R, Ouchi N, Easton RM, Galasso G, Birnbaum MJ, Walsh K, Sessa WC. Akt1/protein kinase Balpha is critical for ischemic and VEGF-mediated angiogenesis. *J Clin Invest*. 2005;115:2119-2127.
  32. Chen WS, Xu PZ, Gottlob K, Chen ML, Sokol K, Shiyanova T, Roninson I, Weng W, Suzuki R, Tobe K, Kadowaki T, Hay N. Growth retardation and increased apoptosis in mice with homozygous disruption of the Akt1 gene. *Genes Dev*. 2001;15:2203-2208.
  33. Pugh CW, Ratcliffe PJ. Regulation of angiogenesis by hypoxia: role of the HIF system. *Nat Med*. 2003;9:677-684.
  34. Cunningham SA, Waxham MN, Arrate PM, Brock TA. Interaction of the Flt-1 tyrosine kinase receptor with the p85 subunit of phosphatidylinositol 3-kinase. Mapping of a novel site involved in binding. *J Biol Chem*. 1995;270:20254-20257.
  35. Igarashi K, Isohara T, Kato T, Shigetani K, Yamano T, Uno I. Tyrosine 1213 of Flt-1 is a major binding site of Nck and SHP-2. *Biochem Biophys Res Commun*. 1998;246:95-99.
  36. Yu Y, Hulmes JD, Herley MT, Whitney RG, Crabb JW, Sato JD. Direct identification of a major autophosphorylation site on vascular endothelial growth factor receptor Flt-1 that mediates phosphatidylinositol 3'-kinase binding. *Biochem J*. 2001;358:465-472.
  37. Roberts DM, Kearney JB, Johnson JH, Rosenberg MP, Kumar R, Bautch VL. The vascular endothelial growth factor (VEGF) receptor Flt-1 (VEGFR-1) modulates Flk-1 (VEGFR-2) signaling during blood vessel formation. *Am J Pathol*. 2004;164:1531-1535.
  38. Kearney JB, Kappas NC, Ellerstrom C, DiPaola FW, Bautch VL. The VEGF receptor flt-1 (VEGFR-1) is a positive modulator of vascular sprout formation and branching morphogenesis. *Blood*. 2004;103:4527-4535.
  39. Bussolati B, Dunk C, Grohman M, Kontos CD, Mason J, Ahmed A. Vascular endothelial growth factor receptor-1 modulates vascular endothelial growth factor-mediated angiogenesis via nitric oxide. *Am J Pathol*. 2001;159:993-1008.
  40. Zeng H, Dvorak HF, Mukhopadhyay D. Vascular permeability factor (VPF)/vascular endothelial growth factor (VEGF) receptor-1 downmodulates VPF/VEGF receptor-2-mediated endothelial cell proliferation, but not migration, through phosphatidylinositol 3-kinase-dependent pathways. *J Biol Chem*. 2001;276:26969-26979.
  41. Hiratsuka S, Nakao K, Nakamura K, Katsuki M, Maru Y, Shibuya M. Membrane fixation of vascular endothelial growth factor receptor 1 ligand-binding domain is important for vasculogenesis and angiogenesis in mice. *Mol Cell Biol*. 2005;25:346-354.
  42. Rosso A, Balsamo A, Gambino R, Dentelli P, Falcioni R, Cassader M, Pegoraro L, Pagano G, Brizzi MF. p53 Mediates the accelerated onset of senescence of endothelial progenitor cells in diabetes. *J Biol Chem*. 2006;281:4339-4347.
  43. Chen Z, Trotman LC, Shaffer D, Lin HK, Dotan ZA, Niki M, Koutcher JA, Scher HI, Ludwig T, Gerald W, Cordon-Cardo C, Pandolfi PP. Crucial role of p53-dependent cellular senescence in suppression of Pten-deficient tumorigenesis. *Nature*. 2005;436:725-730.
  44. Phung TL, Ziv K, Dabhydeen D, Eyiab-Mensah G, Riveros M, Perruzzi C, Sun J, Monahan-Earley RA, Shiojima I, Nagy JA, Lin MI, Walsh K, Dvorak AM, Briscoe DM, Neeman M, Sessa WC, Dvorak HF, Benjamin LE. Pathological angiogenesis is induced by sustained Akt signaling and inhibited by rapamycin. *Cancer Cell*. 2006;10:159-170.
  45. Wang C, Kim H, Hiroi Y, Mukai Y, Satoh M, Liao JK. Increase cellular senescence and cerebral infarct size in mice with chronic activation of endothelial protein kinase Akt. *Circulation*. 2006;114:II-160.
  46. Hojlund K, Staehr P, Hansen BF, Green KA, Hardie DG, Richter EA, Beck-Nielsen H, Wojtaszewski JF. Increased phosphorylation of skeletal muscle glycogen synthase at NH2-terminal sites during physiological hyperinsulinemia in type 2 diabetes. *Diabetes*. 2003;52:1393-1402.
  47. Sheu ML, Ho FM, Yang RS, Chao KF, Lin WW, Lin-Shiau SY, Liu SH. High glucose induces human endothelial cell apoptosis through a phosphoinositide 3-kinase-regulated cyclooxygenase-2 pathway. *Arterioscler Thromb Vasc Biol*. 2005;25:539-545.
  48. Clodfelder-Miller B, De Sarno P, Zmijewska AA, Song L, Jope RS. Physiological and pathological changes in glucose regulate brain Akt and glycogen synthase kinase-3. *J Biol Chem*. 2005;280:39723-39731.
  49. Minamino T, Komuro I. Vascular cell senescence: contribution to atherosclerosis. *Circ Res*. 2007;100:15-26.

# Gremlin Enhances the Determined Path to Cardiomyogenesis

Daisuke Kami<sup>1,3</sup>, Ichiro Shiojima<sup>4</sup>, Hatsune Makino<sup>1</sup>, Kenji Matsumoto<sup>2</sup>, Yoriko Takahashi<sup>1</sup>, Ryuga Ishii<sup>1</sup>, Atsuhiko T. Naito<sup>4</sup>, Masashi Toyoda<sup>1</sup>, Hirohisa Saito<sup>2</sup>, Masatoshi Watanabe<sup>3</sup>, Issei Komuro<sup>4</sup>, Akihiro Umezawa<sup>1\*</sup>

**1** Department of Reproductive Biology, National Institute for Child Health and Development, Tokyo, Japan, **2** Department of Allergy and Immunology, National Institute for Child Health and Development, Tokyo, Japan, **3** Laboratory for Medical Engineering, Division of Materials Science and Chemical Engineering, Graduate School of Engineering, Yokohama National University, Yokohama, Japan, **4** Department of Cardiovascular Science and Medicine, Chiba University Graduate School of Medicine, Chiba, Japan

## Abstract

**Background:** The critical event in heart formation is commitment of mesodermal cells to a cardiomyogenic fate, and cardiac fate determination is regulated by a series of cytokines. Bone morphogenetic proteins (BMPs) and fibroblast growth factors have been shown to be involved in this process, however additional factors need to be identified for the fate determination, especially at the early stage of cardiomyogenic development.

**Methodology/Principal Findings:** Global gene expression analysis using a series of human cells with a cardiomyogenic potential suggested *Gremlin* (*Grem1*) is a candidate gene responsible for *in vitro* cardiomyogenic differentiation. *Grem1*, a known BMP antagonist, enhanced DMSO-induced cardiomyogenesis of P19CL6 embryonal carcinoma cells (CL6 cells) 10–35 fold in an area of beating differentiated cardiomyocytes. The *Grem1* action was most effective at the early differentiation stage when CL6 cells were destined to cardiomyogenesis, and was mediated through inhibition of BMP2. Furthermore, BMP2 inhibited Wnt/ $\beta$ -catenin signaling that promoted CL6 cardiomyogenesis.

**Conclusions/Significance:** *Grem1* enhances the determined path to cardiomyogenesis in a stage-specific manner, and inhibition of the BMP signaling pathway is involved in initial determination of *Grem1*-promoted cardiomyogenesis. Our results shed new light on renewal of the cardiovascular system using *Grem1* in human.

**Citation:** Kami D, Shiojima I, Makino H, Matsumoto K, Takahashi Y, et al. (2008) Gremlin Enhances the Determined Path to Cardiomyogenesis. PLoS ONE 3(6): e2407. doi:10.1371/journal.pone.0002407

**Editor:** Hernan Lopez-Schier, Centre de Regulacio Genomica, Spain

**Received:** January 15, 2008; **Accepted:** May 5, 2008; **Published:** June 11, 2008

**Copyright:** © 2008 Kami et al. This is an open-access article distributed under the terms of the Creative Commons Attribution License, which permits unrestricted use, distribution, and reproduction in any medium, provided the original author and source are credited.

**Funding:** This study was supported by a grant from the Ministry of Education, Culture, Sports, Science and Technology (MEXT) of Japan and Health and Labor Sciences Research Grants; by a Research grant on Health Science Focusing on Drug Innovation from the Japan Health Science Foundation; by the Program for Promotion of Fundamental Studies in Health Science of the Pharmaceuticals and Medical Devices Agency; by a grant from the Terumo Life Science Foundation; by a Research Grant for Cardiovascular Disease from the Ministry of Health, Labor and Welfare (MHLW); and by a Grant for Child Health and Development from the MHLW.

**Competing Interests:** The authors have declared that no competing interests exist.

\* E-mail: umezawa@1985.jukuin.keio.ac.jp

## Introduction

The critical event in heart formation is commitment of mesodermal cells to a cardiomyogenic fate and their migration into anterolateral regions of the embryo during late gastrulation. In this process, morphogenetic movements and cardiac fate determination are regulated by cytokines such as bone morphogenetic proteins (BMPs) [1–3], and fibroblast growth factors (FGFs) [4–7]. These secreted proteins from neighboring endoderm, ectoderm, and the mesoderm itself, play important roles in induction of cardiac transcription factors [8] and differentiation of cardiomyocytes in amphibians [9] and avians [4]. Cardiomyogenic signals, such as BMPs and FGFs, indeed activate expression of cardiac specific transcriptional factors (*Csx/Nkx2.5*, *Gata4*, *Mef2c*), and these transcriptional factors activate expression of circulating hormones (atrial natriuretic peptide (ANP), brain natriuretic peptide (BNP)), and cardiac specific proteins (myosin heavy chain (MyHC), myosin

light chain (MyLC)). Wnt family proteins, cysteine-rich, and secreted glycoproteins, have also been implicated in embryonic development [10,11], and cardiomyogenesis [12,13]. In *Drosophila*, 'wingless', a homologue of vertebrate Wnt is involved in expression of 'tinman', a *Drosophila* homologue of *Csx/Nkx2.5*, through 'armadillo', a *Drosophila* ortholog of  $\beta$ -catenin, and drives heart development [14]. In vertebrates, however, Wnt1/3a, which activates the canonical Wnt/ $\beta$ -catenin signaling pathway leading to stabilization of  $\beta$ -catenin as a downstream molecule through inactivation of glycogen synthase kinase-3 $\beta$ , inhibits cardiomyocyte differentiation from cardiac mesoderm [15–18]. Wnt11 promotes cardiac differentiation via the non-canonical pathway in *Xenopus* [12] and murine embryonic cell lines [19]. The secretion of Wnt inhibitors such as 'Cerberus', 'Dickkopf' and 'Crescent' by the anterior endoderm prevents Wnt3a secreted by the neural tube from inhibiting heart formation [15–17].

In this study, we performed GeneChip analysis to identify multiple extracellular determinants, such as cytokines, cell



membrane-bound molecules and matrix responsible for cardiomyogenic differentiation, and evaluated the statistical significance of differential gene expression by NIA array analysis (<http://lgsun.grc.nia.nih.gov/ANOVA/>) [20], a web-based tool for microarray data analysis. We found that Grem1 enhances the determined path to cardiomyogenesis in a stage-specific manner, and that inhibition of the BMP signaling pathway is, at least in part, involved in initial determination of Grem1-promoted cardiomyogenesis.

## Results

### GeneChip and statistical analysis

To identify cytokines and transcription factors responsible for cardiomyogenic differentiation, 69 human cells were analyzed, depending on gene expression levels, by GeneSpringGX software, and clustered into 30 groups (Fig. 1A, Table 1). Among the 30 groups, 21 groups included cells with a cardiomyogenic potential (Fig. 1B: red numbers). To identify genes specific for these groups, hierarchical clustering was employed, using the average distance method. Genes with the lowest average expression E(G1) within the cluster that can differentiate into cardiomyocytes and genes with the highest average expression E(G2) outside the cluster were identified, as previously described [20–22]. Genes which have  $E(G1) > E(G2)$  were estimated, using the False Discovery Rate ( $FDR < 0.05$ ). Grem1 was nominated as a cluster-specific cardiomyocyte-promoting gene in cells that could differentiate into cardiomyocytes following NIA array analysis (Fig. 1B). The gene expression profile reported in this paper has been deposited in the Gene Expression Omnibus (GEO) database (<http://www.ncbi.nlm.nih.gov/geo>: accession no. GSE8481, GSM41342–GSM41344, and GSM201137–GSM201145).

### Cardiomyogenic differentiation of CL6 cells with Grem1 and DMSO

To investigate cardiomyogenic activity of Grem1, P19CL6 embryonal carcinoma cells (CL6 cells) were used for assessment of *in vitro* cardiomyogenic differentiation, since CL6 cells are reproducibly and stably induced into beating cardiomyocytes by DMSO (Fig. 2Aa) [23]. CL6 cells did not differentiate following exposure to Grem1 alone at concentrations of 63 or 125 ng/ml for 14 days (Fig. 2B). However, Grem1 dramatically promotes DMSO-induced cardiomyogenic differentiation at a concentration of 63 and 125 ng/ml; Grem1 (125 ng/ml) especially increased DMSO-induced cardiomyogenic differentiation of CL6 cells as assessed by beating area (Fig. 2Ab and B) (Movie S1 and S2, <http://1954.jukuin.keio.ac.jp/umezawa/kami/index.html>).

### RT-PCR of differentiated or undifferentiated CL6 cells

To investigate gene expression as well as morphological analysis, i.e. beating, during cardiomyogenic differentiation, RT-PCR analysis was performed to detect expression of cardiomyocyte-specific/associate transcription factors, and structural genes (Fig. 2C). Genes encoding *Cx1/Nkx2.5*, *Gata4*, *Hand2*, *Mef2c*, *ANP*, *BNP*, *MyLC-2a*, *MyLC-2b*, and  $\beta$ -*MyHC* were up-regulated during cardiomyogenic differentiation of CL6 cells treated with Grem1 and DMSO (Fig. 2C: lanes 6, 7 versus lane 3). Triplicate independent experiments confirmed the concentration-dependent Grem1 action on cardiomyogenic differentiation. The cardiomyocyte-specific genes (*Cx1/Nkx2.5*, *Gata4*, *MyLC-2a*, *MyLC-2b*) expression level of CL6 cells treated with DMSO and Grem1 (63 and 125 ng/ml) were also the same as or higher than that of DMSO-induced CL6 cells by semi-quantitative RT-PCR (Figure S1).

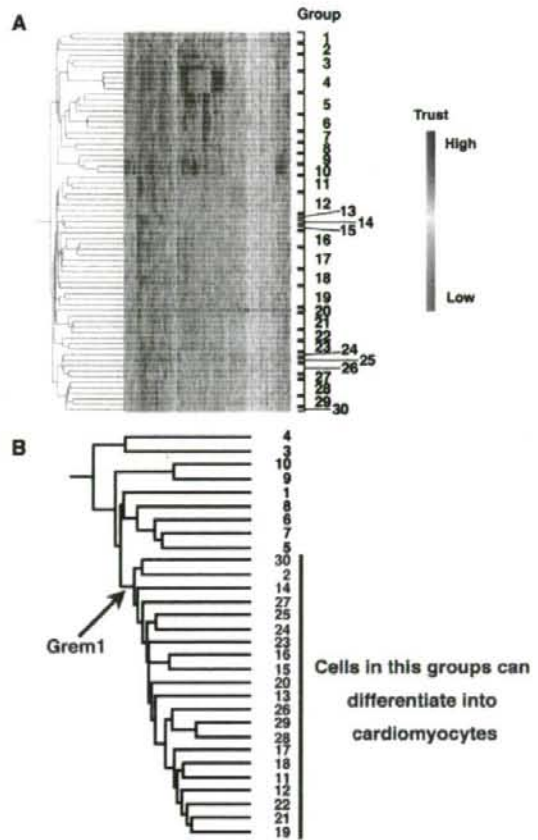


**Figure 1. Hierarchical clustering analysis on cultured human cells. (A)** Hierarchical clustering analyzed by GeneSpring. Based on gene expression pattern, 69 human cells were clustered into 30 sub-groups. The raw data from the GeneChip analysis are available at the GEO database with accession number GSE8481, GSM41342–GSM41344, and GSM201137–GSM201145. **(B)** Hierarchical clustering analysis was performed by NIA array (<http://lgsun.grc.nia.nih.gov/ANOVA/>), using averaged values of 30 sub-groups. Among the 30 groups, 21 groups included cells with a cardiomyogenic potential. To identify genes specific for these groups, hierarchical clustering was employed. Grem1 was nominated as a cluster-specific cardiomyocyte-promoting gene in cells that could differentiate into cardiomyocytes. doi:10.1371/journal.pone.0002407.g001

### Immunocytochemistry of differentiated or undifferentiated CL6 cells

To examine CL6 cells for expression of cardiomyocyte protein, immunocytochemical analysis was performed. CL6 treated with Grem1 (125 ng/ml) and DMSO exhibited clear striation with immunostain using anti-cTnT or anti- $\alpha$ -actinin (Fig. 2Da and b). The MF20- and cTnT-positive cells after exposure to Grem1 and DMSO formed clusters (Fig. 2Ea), compared with the cells after exposure to DMSO alone (Fig. 2Eb). CL6 cells treated with Grem1 alone were negative for MF20 and cTnT, but became positive for both markers following exposure to Grem1 (63 and 125 ng/ml) and DMSO (Fig. 2F). The beating area (Fig. 2B) showed a tendency similar to the MF20- and cTnT-positive area (Fig. 2F), thus there were positive correlations between them.

**Table 1.** 69 human cells clustered into 30 groups

Group	Title	Description	GSM	
1	Normal epithelial cell, primary	NHEK-Neo1	Normal epidermal keratinocyte, neonate, primary	GSM210361
		NHBE-1	Normal bronchial epithelial cell, primary	GSM210362
2	Pulmonary epithelial cell line	A549	Pulmonary epithelial cell line	GSM210363
		BEAS-2B control (6hr)	Bronchial epithelial cell line	GSM210364
3	Lymphocyte	RPMI8226control (6hr)	B cell line	GSM210365
		Raji-1	B cell line	GSM210366
		NK92	NK cell line	GSM210367
4	Myelomonocytic leukemia	U937c	U937 control	GSM210368
		U937h	U937+HRF	GSM210369
		U937ha	U937+HRF+antibody	GSM210370
		U937a	U937+antibody	GSM210371
5	Embryonal carcinoma, cancer	NCR-G3	Embryonal carcinoma, NCR-G3, non-adherent	GSM201141
		NCR-G2NAd	Embryonal carcinoma, NCR-G2, non-adherent	GSM210373
		NCR-G4Ad	Embryonal carcinoma, NCR-G4, adherent	GSM201142
		NCR-G3Ad	Embryonal carcinoma, NCR-G3, adherent	GSM210375
6	ES cell	H1_P43	Undifferentiated hES	GSM41342
		H1-P46	Undifferentiated hES	GSM41343
		H1-P41	Undifferentiated hES	GSM41344
		NCR-G2Ad	Embryonal carcinoma, NCR-G2, adherent	GSM201140
7	Embryonal carcinoma, cancer	NCR-G1	Embryonal carcinoma, NCR-G3, non-adherent	GSM201139
		NCR-EW2	Ewing, cancer	GSM210378
8	Ewing, cancer	NCR-EW3	Ewing, ETV4, cancer	GSM210379
		GST6	Ewing, POU5F1, cancer	GSM201137
9	Ewing, cancer	GST6-extra	Ewing, POU5F1, cancer	GSM210381
		GST6-Saz	Ewing, POU5F1, SazaC, cancer	GSM201138
10	Ewing, cancer	GST6-Saz-extra	Ewing, POU5F1, SazaC, cancer	GSM210383
		H4-1	Bone marrow cell, primary	GSM201143
11	Bone marrow cell, primary	UBT5	Bmi-1, hTERT, bone marrow cell	GSM210385
		UBET7	Bmi-1, E6, hTERT, bone marrow cell	GSM210386
		#10	Ligament, primary	GSM210387
12	Ligament-derived cells	H10-2Vec	Vector, bone marrow cell	GSM210388
		H10-2TERT	hTERT, bone marrow cell	GSM210389
		H10-2Bmi1	Bmi-1, bone marrow cell	GSM210390
13	Placenta, primary	PL90	Placenta, primary	GSM210391
14	De-differentiated chondrocyte	TdHC1	E6, E7, hTERT, de-differentiated chondrocyte	GSM210392
15	Neural differentiated marrow stromal cell	UET13 Neural differentiation	E7, hTERT, neural differentiation, bone marrow cell	GSM210393
16	Neural differentiated marrow stromal cell	UET13 Neural differentiation1	E7, hTERT, neural differentiation, bone marrow cell	GSM210394
		UET13 Neural differentiation4	E7, hTERT, neural differentiation, bone marrow cell	GSM210395
		UET13 Neural differentiation5	E7, hTERT, neural differentiation, bone marrow cell	GSM210396
17	Cord blood-derived cells	UET13	E7, hTERT, bone marrow cell	GSM210397
		UCB408	Cord blood, primary	GSM210398
		UCB408E6E7-31	E6, E7, umbilical cord blood	GSM210399
		HAdpc1E6E7TERT8	HAdpc1E6E7TERT8	GSM210400
18	Adipocyte cell, primary	UEET12	E6, E7, hTERT, bone marrow cell	GSM210401
		UEE16	E6, E7, bone marrow cell	GSM210402
		EPC hTERT+1	E6, E7, hTERT, endometrial cell	GSM201144
19	Cord blood, primary	UCB302	Cord blood, primary	GSM210382
		UCB302-D7	Cord blood, primary	GSM210405
		UCB302TERT	hTERT, cord blood	GSM210406
		UET9	E7, hTERT, bone marrow cell	GSM210407



Table 1. cont.

Group	Title	Description	GSM	
20	Cord blood, primary	UCB408E7-32	E7, hTERT, cord blood	GSM210408
21	Fetal fibroblast, primary	HFDPC cont.	Normal follicular dermal papillar cell, primary	GSM210409
		PL112	Placenta, primary	GSM210410
		HF7-3	Fetal fibroblast, primary	GSM210411
22	Bone marrow cell, primary	3F0664	Bone marrow cell (commercial item), primary	GSM201145
		BM-MSK	Bone marrow-derived mesenchymal stem cells	GSM38627
23	ES cell-derived mesenchymal cell	H1 clone 2	ES cell-derived mesenchymal precursor	GSM38628
		H9 clone 1	ES cell-derived mesenchymal precursor	GSM38629
24	Endometrial cell	EPC100	E6, E7, hTERT, endometrial cell	GSM210413
25	Bone marrow cell, primary	Yub10F	Bone marrow cell, primary	GSM210414
26	Endometrial cell	EPC hTERT+2	E6, E7, hTERT, endometrial cell	GSM210415
		EPC Control	E6, E7, hTERT, endometrial cell	GSM210416
27	Endometrial cell	EPC214	E6, E7, hTERT, endometrial cell	GSM210417
28	Menstruation blood-derived mesenchymal cell, primary	#E4	Menstruation blood, primary	GSM210418
		#E4HRF	Menstruation blood, HRF treatment, primary	GSM210419
		#ESHFRF	Menstruation blood, HRF treatment, primary	GSM210420
29	Menstruation blood-derived mesenchymal cell, primary	#E6	Menstruation blood, primary	GSM210421
		#E6HRF	Menstruation blood, HRF treatment, primary	GSM210422
30	Menstruation blood-derived mesenchymal cell, primary	#ES	Menstruation blood, primary	GSM210423

doi:10.1371/journal.pone.0002407.t001

### Grem1 and DMSO were most effective at the early stage (days 1–3) of CL6 differentiation

To determine if Grem1 (125 ng/ml) functions during the early or the late stage of differentiation, CL6 cells were treated with Grem1 for different time periods (Fig. 3A). Grem1 and DMSO were most effective on CL6 differentiation at 1–3 days (Fig. 3B, C) as assessed by percentages of MF20-positive area and beating area. Since Grem1 inhibits BMPs through direct binding [24], we hypothesized that BMP signaling is inhibitory to CL6 cardiomyogenesis during days 1–3. To confirm this hypothesis, RT-PCR analysis was performed to determine expression of the early mesodermal marker (*BrachyuryT* and *Tbx6*), cardiomyocyte-specific transcription factors (*Cx1/Nx2.5*), structural genes ( *$\beta$ -MyHC*), and *Gapdh* (Fig. 4A). DMSO induced the *BrachyuryT* and *Tbx6* genes, and their expressions peaked at 3 days and then decreased; BMP2 down-regulated expression of these genes at 3–7 days. The *Cx1/Nx2.5* and  *$\beta$ -MyHC* genes started to be expressed at days 3 and 5, respectively, and their expression increased up to 14 days, at which time the timeframe analysis was terminated. BMP2 clearly inhibited expression of the *Cx1/Nx2.5* and  *$\beta$ -MyHC* genes (Fig. 4A, lanes 1–7 versus lanes 8–14).

To examine cardiomyogenic differentiation, immunocytochemical analysis was performed on CL6 cells treated with the inducers. CL6 cells treated with DMSO and BMP2 for the first 3 days were negative for sarcomeric myosin (MF20) at 14 days, but became positive for sarcomeric myosin, following exposure to DMSO alone during days 1–3 (Fig. 4B). To determine if DMSO induces BMP production in CL6 cells, expression levels of *Bmp2* and *Bmp4* were determined by quantitative real-time RT-PCR analysis (Fig. 4C). DMSO clearly induced the *Bmp2* and *Bmp4* genes, and

DMSO-induction was inhibited by BMP2 protein. The expression level of *Bmp2* was highest during days 7–10 (Fig. 4C: *Bmp2*) in DMSO-induced CL6 cells, and that of *Bmp4* was highest during days 5–7 (Fig. 4C: *Bmp4*).

To investigate BMP signaling on cardiomyogenic differentiation, we used the *Id1* promoter-Lux plasmid that includes the luciferase gene driven by the *Id1* promoter, known as a BMP target promoter (Fig. 4D). DMSO increased BMP signaling activity that peaked at 5 days (Fig. 4D, open square). BMP2 protein increased BMP signaling activity at 3 days (Fig. 4D, closed square), but lost BMP signaling activity at 5 days and later, implying that this loss of BMP signaling leads to lack of cardiomyogenic induction.

Since Wnt/ $\beta$ -catenin signaling is involved in CL6 cardiomyogenesis [23,25], we hypothesized that the BMP effect on CL6 cardiomyogenesis is mediated through Wnt/ $\beta$ -catenin signaling. Expression of *Wnt3a*, an activator of canonical Wnt signaling, was indeed detected in CL6 cells exposed to DMSO, and BMP2 significantly down-regulated *Wnt3a* expression at day 3 (Fig. 4E). By using the TOPflash plasmid [23] which includes the luciferase gene driven by two sets of three copies of the TCF recognition site, Wnt/ $\beta$ -catenin signaling activity increased at 48 h after treatment with DMSO. Activity was increased by DMSO treatment but decreased by BMP2 (Fig. 4F). Time course analysis revealed that Wnt/ $\beta$ -catenin activity peaked at 5 days after DMSO treatment, and decreased thereafter (Fig. 4G). BMP2 inhibited DMSO-induced Wnt/ $\beta$ -catenin activity throughout the experimental period (up to 14 days). These results imply that BMP signaling inhibits CL6 cardiomyogenesis at the early stage through inhibition of Wnt/ $\beta$ -catenin signaling.

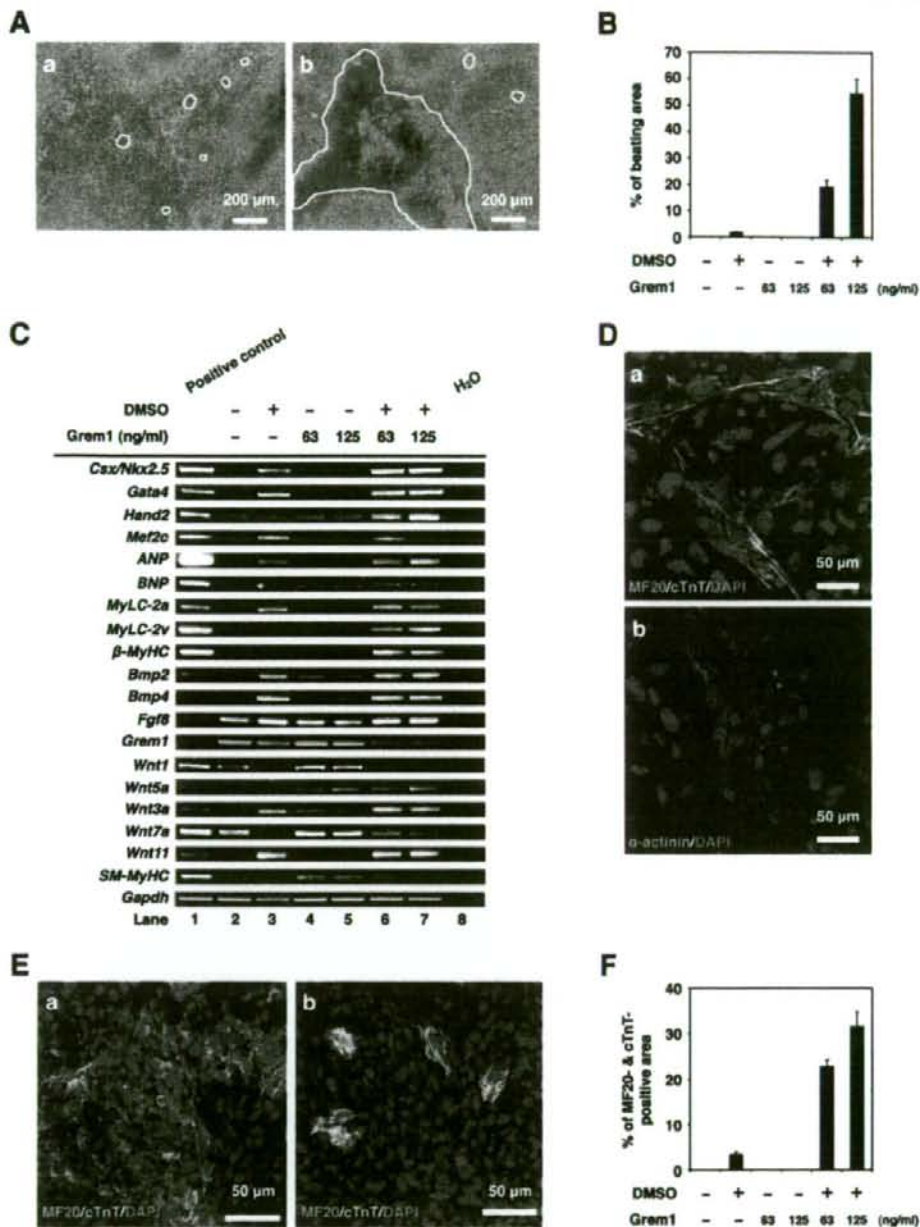


**Figure 2. Grem1 enhanced cardiomyogenic differentiation in DMSO-induced CL6 cells.** (A) Phase contrast micrograph of CL6 cells with exposure to DMSO alone (a), Grem1 (125 ng/ml) and DMSO (b) for 14 days. The medium, including Grem1 and DMSO, was changed every day. CL6 cells exhibited apparent spontaneous beating between days 9–11. Beating CL6 cell colonies are outlined by white lines. (B) Percentage of beating area in differentiated CL6 cells. CL6 cell treated with Grem1 (125 ng/ml) and DMSO exhibited the strongest contraction. (C) RT-PCR analysis of the genes encoding cardiac-specific transcriptional factors (*Cx3/Nkx2.5*, *Gata4*, *Mef2c*, *Hand2*), circulating hormone (*ANP*, *BNP*), cardiac-specific proteins (*MyLC-2a*, *MyLC-2v*,  $\beta$ -MyHC), cytokines (*Bmp2*, *Bmp4*, *Fgf8*, *Grem1*, *Wnt1*, *Wnt3a*, *Wnt5a*, *Wnt7a*, *Wnt11*), SM-MyHC, and *Gapdh* (From top to bottom). Mouse total heart RNA for the *Cx3/Nkx2.5*, *Gata4*, *Mef2c*, *Hand2*, *ANP*, *BNP*, *MyLC-2a*, *MyLC-2v*,  $\beta$ -MyHC, *Bmp2*, *Bmp4*, *Grem1*, *Wnt1*, *Wnt3a*, *Wnt5a*, *Wnt7a*, *Wnt11*, SM-MyHC, and *Gapdh* genes, mouse embryonic stem cell RNA for the *Fgf8* gene, and mouse total skeletal muscle RNA for the *Wnt1*, *Wnt3a*, *Wnt5a*, and *Wnt7a* genes were used for positive controls. H<sub>2</sub>O (without RNA) served as a negative control. (D) Immunocytochemistry of CL6 cells 14 days after exposure to Grem1 (125 ng/ml) and DMSO with MF20 and cTnT (a), and  $\alpha$ -actinin (b). Cell nuclei are stained with DAPI. Clear striations are evident. (E) Immunocytochemistry of CL6 cells 14 days after exposure to Grem1 and DMSO with cardiac troponin T (cTnT) and sarcomeric myosin (MF20). CL6 cells treated with Grem1 (125 ng/ml) and DMSO (a), and DMSO alone (b) stained positive for cTnT and MF20. Untreated CL6 cells, i.e. not exposed to Grem1 (125 ng/ml) or DMSO, stained negative for cTnT and MF20. Cell nuclei were stained with DAPI. (F) Percentage of MF20- and cTnT-double positive area.

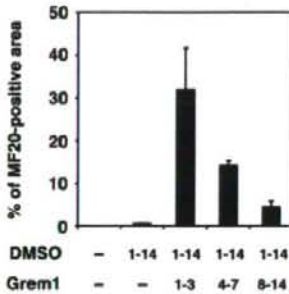
doi:10.1371/journal.pone.0002407.g002



A

Day	0	1	2	3	4	5	6	7	8	9	10	11	12	13	14
DMSO	-	-	-	-	-	-	-	-	-	-	-	-	-	-	-
Grem1	-	-	-	-	-	-	-	-	-	-	-	-	-	-	-
DMSO 1-14	-	+	+	+	+	+	+	+	+	+	+	+	+	+	+
Grem1	-	-	-	-	-	-	-	-	-	-	-	-	-	-	-
DMSO 1-14	-	+	+	+	+	+	+	+	+	+	+	+	+	+	+
Grem1 1-3	-	+	+	+	-	-	-	-	-	-	-	-	-	-	-
DMSO 1-14	-	+	+	+	+	+	+	+	+	+	+	+	+	+	+
Grem1 4-7	-	-	-	-	+	+	+	+	-	-	-	-	-	-	-
DMSO 1-14	-	+	+	+	+	+	+	+	+	+	+	+	+	+	+
Grem1 8-14	-	-	-	-	-	-	-	-	+	+	+	+	+	+	+
DMSO 1-3	-	+	+	+	-	-	-	-	-	-	-	-	-	-	-
Grem1	-	-	-	-	-	-	-	-	-	-	-	-	-	-	-
DMSO 1-14	-	+	+	+	+	+	+	+	+	+	+	+	+	+	+
Grem1 1-14	-	+	+	+	+	+	+	+	+	+	+	+	+	+	+
DMSO 1-14	-	+	+	+	+	+	+	+	+	+	+	+	+	+	+
Grem1 1-3	-	+	+	+	-	-	-	-	-	-	-	-	-	-	-
DMSO 1-3	-	+	+	+	-	-	-	-	-	-	-	-	-	-	-
Grem1 1-3	-	+	+	+	-	-	-	-	-	-	-	-	-	-	-

B



C

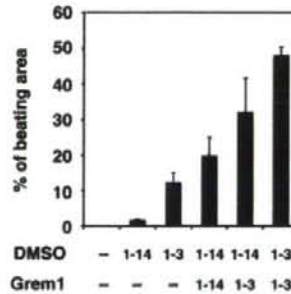


**Figure 3. Percentage of myogenic differentiation by period of treatment with Grem1 in CL6 cells. (A)** Protocol for treatment of Grem1 and DMSO. CL6 cells were passaged at  $1.8 \times 10^5$  cells in 6-well plate on Day 0. CL6 cells were exposed to Grem1 (125 ng/ml) and/or DMSO on the indicated day. Day when the cells were exposed to the inducers is shown by "+" (in gray cells for clarity). The medium including Grem1 and DMSO was changed every day. On day 14, the cells were immunocytochemically stained with MF20 antibody. **(B)** Myogenic differentiation of CL6 cells was estimated by sarcomeric myosin (MF20)-positive area. CL6 cells were treated with Grem1 (125 ng/ml) and DMSO for the indicated days. **(C)** Myogenic differentiation of CL6 cells was estimated by beating area. CL6 cells treated with DMSO and Grem1 (125 ng/ml) were incubated at indicated days. doi:10.1371/journal.pone.0002407.g003

## Discussion

Our bioinformatics study using the results from the global gene expression analysis of human cells (GSM412342-41344 and GSM201137-201145 at <http://www.ncbi.nlm.nih.gov/geo>) nominated Grem1 as a candidate gene that may participate in cardiomyogenesis. By using CL6 embryonic cells as a model of cardiomyogenesis, we obtained two major findings: the first is that Grem1 enhanced cardiomyogenic differentiation of DMSO-induced CL6 cells at the early stage; the second is that Wnt/ $\beta$ -catenin and BMP signaling activity had developmental stage-specific effects on cardiomyogenesis (Fig. 5). Wnt/ $\beta$ -catenin activity at the early stage enhanced embryonic cell differentiation into cardiomyocytes, while suppressing this activity by BMP2 or BMP4 proteins as reported in the avian embryo [26]. In contrast, BMP signaling activity in the late stage enhanced cardiomyogenic

differentiation. Grem1 regulated the stage-specific Wnt/ $\beta$ -catenin and BMP signaling activity on cardiomyogenesis.

Many studies have indicated that Grem1 is involved in cell differentiation and development, such as osteogenesis [27], lung morphogenesis [28], myogenesis [29], and limb formation [30], through inhibition of BMP2 and BMP4. Grem1-null mice show intact heart development, despite impairment of lung and kidney [31], and therefore Grem1 is considered not to be involved in cardiogenesis, or supplementary factors such as Noggin [32], with a similar function, may compensate Grem1 during development. Grem1 had an enhancing or promoting activity in *in vitro* cardiomyogenesis, as is the case with platelet-derived growth factor as a promoter of cell growth [33]. In this study, Grem1 was involved in cardiomyocyte differentiation. However Grem1 alone could not induce cardiomyocytic differentiation of CL6 cells in the absence of DMSO (Fig. 2C and F), suggesting that Grem1 is solely

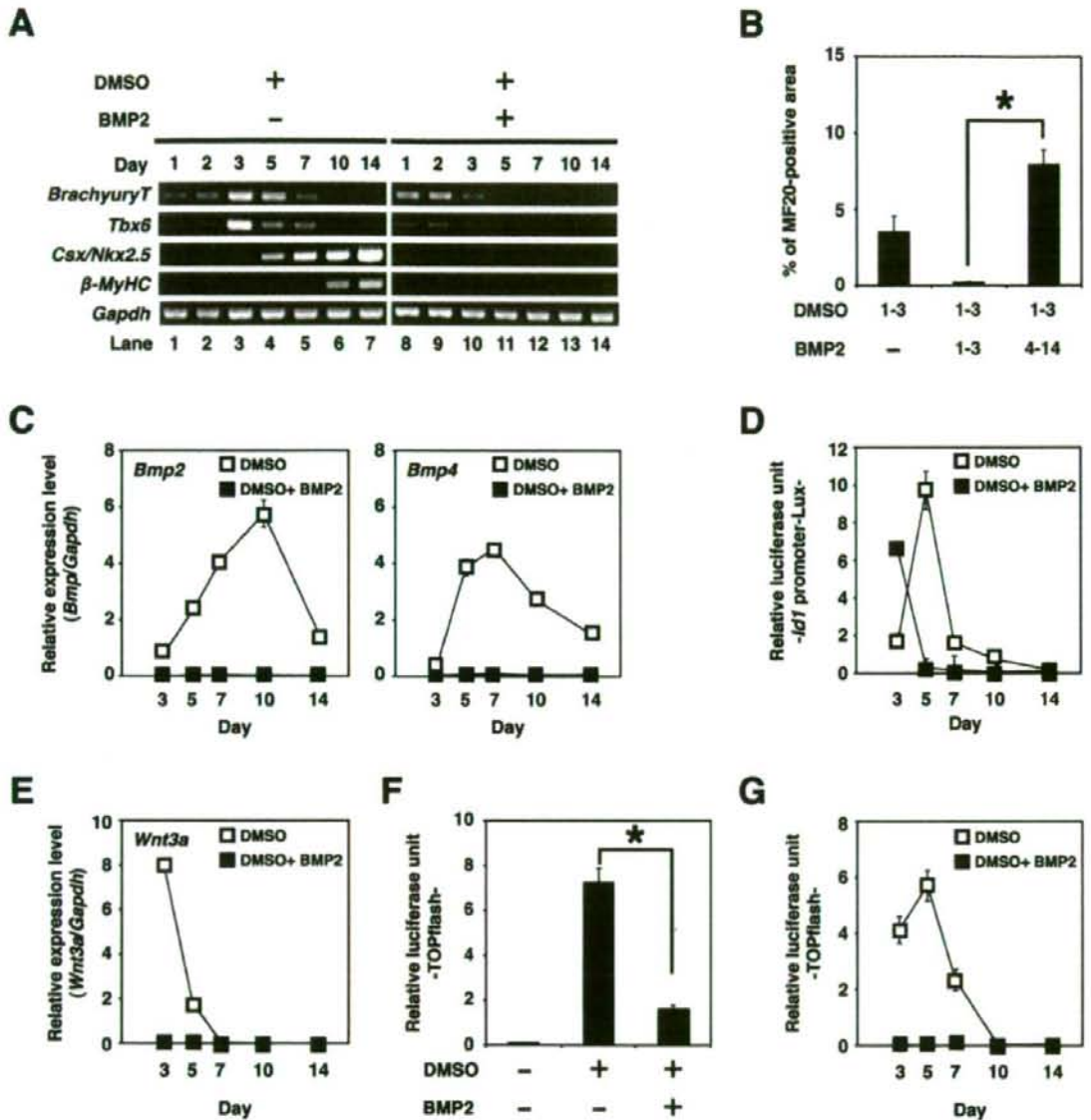


**Figure 4. Cardiomyogenic differentiation in CL6 cells (days 1–3) is inhibited by BMP2.** (A) RT-PCR analysis of the gene encoding *BrachyuryT*, *Tbx6*, cardiac-specific transcriptional factor (*Csx/Nkx2.5*), cardiac-specific protein ( $\beta$ -MyHC), and *Gapdh* (From top to bottom) of CL6 cells treated with DMSO alone, or DMSO and BMP2 (100 ng/ml) for the first 3 days (days 1–3). The medium, including BMP2 and DMSO, was changed every day. (B) Percentage of MF20-positive area. Immunocytochemistry was carried out on CL6 cells 14 days after cells had been exposed to DMSO and BMP2 (100 ng/ml) for the first 3 days (days 1–3). The asterisk indicates a significant statistical difference ( $P < 0.05$ ). (C) Quantitative real-time RT-PCR analysis of the gene encoding *Bmp2* (left), and *Bmp4* (right) in CL6 cells treated with DMSO alone (open square), or DMSO and BMP2 (100 ng/ml) (closed square) for the first 3 days (days 1–3). (D) BMP signaling activity of CL6 cells treated with DMSO alone (open square), or DMSO and BMP2 (100 ng/ml) (closed square) for the first 3 days (days 1–3) were determined by luciferase activity analysis using *Id1* promoter-Lux (a firefly luciferase reporter plasmid driven by the *Id1* binding sites), pRL-CMV as co-transfected control, and Dual luciferase reporter assay system. Relative luciferase unit of the CL6 cells untreated with inducers at day 3 is regarded as 0.1 (data not shown). (E) Quantitative real-time RT-PCR analysis of the gene encoding *Wnt3a* in CL6 cells treated with DMSO alone (open square), or DMSO and BMP2 (100 ng/ml) (closed square) for the first 3 days (days 1–3). (F) Wnt/ $\beta$ -catenin signaling activity of CL6 cells 48 h after exposure to DMSO, or DMSO and BMP2 (100 ng/ml) was determined by luciferase activity analysis using TOPflash (a firefly luciferase reporter plasmid driven by two sets of three copies of the TCF binding site and herpes simple virus thymidine kinase minimal promoter), pRL-CMV as co-transfected control, and Dual luciferase reporter assay system. Relative luciferase unit of the CL6 cells untreated with inducers is regarded as 0.1. The asterisk indicates a significant statistical difference ( $P < 0.05$ ). (G) Timeframe of Wnt/ $\beta$ -catenin signaling activity in CL6 cells treated with DMSO alone (open square), or DMSO and BMP2 (100 ng/ml) (closed square) for the first 3 days (days 1–3). Relative luciferase unit of the CL6 cells untreated with inducers at day 3 is regarded as 0.1 (data not shown). doi:10.1371/journal.pone.0002407.g004



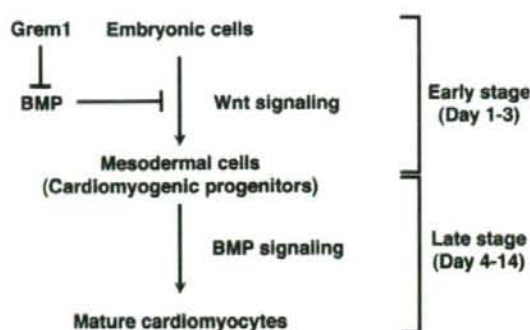


**Figure 5. Grem1-accelerated CL6 cardiomyogenesis through regulation of BMP- and Wnt/ $\beta$ -catenin-signaling pathways.** CL6 embryonic cells start to differentiate into mesodermal cells through Wnt/ $\beta$ -catenin signaling pathway at the early stage (days 1–3), and mesodermal CL6 cells differentiate into mature cardiomyocytes by BMP pathway at the late stage (days 4–14). Grem1 accelerates DMSO-induced cardiomyogenesis through inhibition of the BMP-signaling pathway. doi:10.1371/journal.pone.0002407.g005

a promoter of cardiomyogenic differentiation. One of the possible mechanisms for Grem1-enhanced cardiomyogenesis at the early stage is inhibition of the BMP signaling pathway [3]. Alternatively, Grem1-enhanced cardiomyogenesis may be mediated through proliferation of cardiac progenitor cells, as is the case of myogenic progenitor proliferation by Grem1 [34], and this possibility is supported by an increased number of sarcomeric myosin-positive CL6 cardiomyocytes (Fig. 2E and F).

The stage specificity of the Grem1 effect is possibly correlated with the biphasic and antagonistic effect of Wnt/ $\beta$ -catenin signaling on cardiomyogenesis, depending on the stage of development *in vitro* [25] and *in vivo* [35]. CL6 cells differentiated into cardiomyocytes via mesodermal induction by the Wnt/ $\beta$ -catenin signaling pathway at the early stage, and CL6 mesodermal cells differentiated into cardiomyocytes induced by BMP2 at the late stage. It is conceivable that embryonic cells, such as CL6 cells and ES cells, differentiate into cardiomyocytes by inhibiting BMP signaling via putative “mesodermal cells” or “cardiomyogenic progenitors”, or differentiation stages corresponding to these cells (Fig. 5, Figure S2). The early stage process from embryonic cells to mesodermal cells was mediated via Wnt/ $\beta$ -catenin signaling (Fig. 4F, G), and was assessed by expression of *BrachyuryT* and *Tbx6* genes (Fig. 4A), which are target genes for Wnt/ $\beta$ -catenin signaling [36]. BMP signaling antagonizes the cell fate-inducing activity of Wnt/ $\beta$ -catenin [37]. When embryonic cells or cardiomyogenic progenitors are induced to become mature cardiomyocytes by cytokines and growth factors, we must be careful with respect to the stage of cell differentiation because of the biphasic differential action of the factors which are dependent upon the differentiation stage.

In conclusion, we have demonstrated that Grem1 enhances the commitment or determined path to cardiogenic differentiation of CL6 teratocarcinoma cells. Apart from a role in development, Grem1 may serve a clinical use in cardiology, like granulocyte colony-stimulating factor that accelerates production of granulocytes in both peripheral blood and bone marrow. Nomination of *Grem1* as a cardiomyogenic factor is based on hierarchical clustering analysis using global gene expression data of human cells. This bioinformatics approach may be useful for identifying morphogens/factors that can induce differentiation of other cell types/tissues/organs.

## Materials and Methods

### GeneChip analysis

GeneChip analysis was performed (Fig. 1A, Table 1) as previously described [38]. Human genome-wide gene expression was examined with the Human Genome U133A Probe array (GeneChip; Affymetrix), which contains the oligonucleotide probe set for approximately 23,000 full-length genes and expressed sequence tags, according to the manufacturer's protocol (Expression Analysis technical manual and GeneChip Small Sample Target Labeling Assay version 2 technical note [http://www.affymetrix.com/support/technical/index.affx]). Data analysis was performed by the GeneChip Operation System (Affymetrix) and GeneSpringGX software (Silicon Genetics). To normalize the staining intensity variations between chips, the average difference values for all genes on a given chip were divided by the median of all measurements on that chip. Hierarchical-clustering analysis was performed using a minimum distance value of 0.001, a separation ratio of 0.5, and the standard definition of the correlation distance.

### Cell culture and differentiation

CL6 cells were grown on 100 mm dishes (Becton Dickinson) in  $\alpha$ -MEM (Gibco) supplemented with 10% fetal bovine serum (FBS) (JRH Bioscience, Inc.), penicillin, and streptomycin, and were maintained in a 5% CO<sub>2</sub> atmosphere at 37°C. To induce differentiation, CL6 cells were plated at a density of  $1.8 \times 10^5$  cells in a 6-well plate (Becton Dickinson) or gelatin-coated 35 mm glass base dishes (IWAKI) with  $\alpha$ -MEM containing Grem1 (63 or 125 ng/ml; R&D system) and/or 1% dimethyl sulfoxide (DMSO) for 14 days. Recombinant human bone morphogenetic protein-2 (BMP2) was purchased from R&D systems.

### Reverse transcriptase-PCR (RT-PCR) and quantitative real-time RT-PCR analysis

Total RNAs were extracted from differentiated and undifferentiated CL6 cells and mouse embryonic stem (ES) cells with RNeasy minikit and DNase I treatment (QIAGEN). Mouse ES cell (129 strains) RNA, mouse heart total RNA (Clontech) and mouse skeletal muscle/total RNA (UNITTECH. Co., Ltd.) were used as a positive control for each primer. Total RNA (2.0  $\mu$ g each) for RT-PCR was converted to cDNA with Superscript<sup>TM</sup> III RNase H<sup>-</sup> reverse transcriptase (Invitrogen), according to the manufacturer's manual. PCR conditions were optimized and linear amplification range was determined for each primer by varying annealing temperature and cycle number. PCR products were identified by positive control size. RT-PCR was performed using the primers of the genes of cardiac specific transcription factors: *Cx36/Nkx2.5*, *Gata4*, *Mef2c*, *Hand2*; circulating hormone: *ANP*, *BNP*; cardiac structural proteins:  $\beta$ -MyHC, *MyLC-2a*, *MyLC-2v*; cytokines: *Bmp2*, *Bmp4*, *Fgf8*, *Grem1*, *Wnt1*, *Wnt3a*, *Wnt5a*, *Wnt7a*, *Wnt11*; smooth muscle structural protein: smooth muscle-myosin heavy chain (*SM-MyHC*); the early mesodermal marker: *BrachyuryT*, *T-box6* (*Tbx6*); and *Gapdh* as control. PCR was performed with exTaq DNA polymerase and exTaq PCR buffer (TaKaRa) or LATaq DNA polymerase and GC buffer I (TaKaRa) for 25 or 30 cycles, with each cycle consisting of 95°C for 30 s, 50°C, 55°C, 60°C or 65°C for 45 s, and 72°C for 45 s, with an additional 5 min incubation at 72°C after completion of the final cycle. PCR primers for the genes of *Cx36/Nkx2.5*, *Gata4*, *Mef2c*, *Hand2*, *ANP*, *BNP*,  $\beta$ -MyHC, *MyLC-2a*, *MyLC-2v*, *Bmp2*, *Bmp4*, *Fgf8*, *Grem1*, *Wnt1*, *Wnt3a*, *Wnt5a*, *Wnt7a*, *Wnt11*, *SM-MyHC*, *BrachyuryT*, *Tbx6*, and *Gapdh* (Table S1a) were obtained from Mouse Genome



Informatics (<http://www.informatics.jax.org/>). The PCR products were size-fractionated by 2% agarose gel electrophoresis.

Quantitative real-time RT-PCR was performed on an ABI Prism 7700 Sequence Detection System (Applied Biosystems), using 100 ng of cDNA in 25  $\mu$ l reaction volume with 10 nmol/l of each primer, and 12.5  $\mu$ l SYBR Green Realtime PCR Master Mix (TOYOBO). PCR primers for the genes of *Bmp2*, *Bmp4*, *Wnt3a*, and *Gapdh* (Table S1b) were obtained from PrimerBank (<http://pga.mgh.harvard.edu/primerbank/index.html>). Calculations were automatically performed by ABI software (Applied BioSystems).

### Immunocytochemistry

A laser confocal microscope (LSM510, Zeiss) was used for immunocytochemical analysis. Differentiated and undifferentiated CL6 cells were fixed with 4% paraformaldehyde (Wako) for 5 min at 4°C and treated with 0.1% Triton X-100 (Sigma) in PBS for 20 min at room temperature, then incubated for 20 min at room temperature in a protein-blocking solution consisting of PBS supplemented with 5% normal goat serum (DakoCytomation). These CL6 cells were then incubated overnight with primary antibody monoclonal anti-sarcomeric myosin antibody (MF20, mouse IgG<sub>2b</sub> isotype, 1 mg/ml, University of Iowa Hybridoma Bank) and Troponin T, and Cardiac Isoform Ab-1 clone 13-11 (cTnT, mouse IgG<sub>1</sub> isotype, 1:300, Lab Vision Corp), or the monoclonal anti- $\alpha$ -actinin (SARCOMERIC) CLONE EA-53 ( $\alpha$ -actinin, mouse IgG<sub>1</sub> isotype, 1:300, Sigma) in PBS at 4°C. The cells were extensively washed in PBS and incubated at room temperature with Alexa Fluor 568-conjugated goat anti-mouse IgG<sub>2b</sub> (anti-MF20) (Molecular Probe; diluted 1:300), Alexa Fluor 488-conjugated goat anti-mouse IgG<sub>1</sub> (anti-cTnT) (Molecular Probe; diluted 1:300), Alexa Fluor 546-conjugated goat anti-mouse IgG(H+L) (anti- $\alpha$ -actinin) (Molecular Probe; diluted 1:300), and nuclei were counterstained with 4', 6-diamidino-2-phenylindole (DAPI) (Wako; diluted 1:300) for 45 min. To prevent fading, cells were then mounted in DakoCytomation Fluorescent Mounting Medium (DakoCytomation).

### Transfection and luciferase assays

Cells ( $8.0 \times 10^5$ ) seeded and cultured in 60 mm dishes (Becton Dickinson) were transfected 18 h after plating using Lipofectamine 2000 (Invitrogen) and PLUS reagent (Invitrogen) in Opti-MEM (Gibco). Transfection contained 1.0  $\mu$ g of TOPflash plasmid (Upstate Biotechnology) for measurement of Wnt/ $\beta$ -catenin activity, or 5.0  $\mu$ g of the *Id1* promoter-Lux plasmid (provided by Dr Imamura and Dr Miyazono) for measurement of BMP-induced *Id1* gene transcription, and 0.5  $\mu$ g of pRL-CMV (Promega) as co-transfected control. Medium containing 10% FBS was changed 3 h after transfection and transfected cells ( $1.8 \times 10^5$ ) were re-seeded in 6-well plates 24 h after transfection. After 18 h, CL6 cells were induced with BMP2 (100 ng/ml) and DMSO. CL6 cells were prepared for luciferase activity analysis using Dual luciferase reporter assay system (Promega).

### Area calculation

The regions of interest (beating area, immunostaining area) were defined in Photoshop (Adobe systems) using the 'magic wand' tool. The total numbers of pixels identified were then counted using the histogram function. At least five different fields were measured for each dish.

### Statistical analysis

Results, shown as the mean  $\pm$  SE, were compared by ANOVA followed by Scheffé's test, with  $P < 0.05$  considered significant.

## Supporting Information

**Figure S1** A semi-quantitative RT-PCR of cardiomyocyte-specific genes. To investigate expression level of cardiomyocyte-specific genes (*Cx36/Nkx2.5*, *Gata4*, *MyLC-2a*, and *MyLC-2v*), a semi-quantitative RT-PCR was performed from CL6 cells treated with 1% DMSO and the indicated concentration of Grem1 for 14 days. Each RT-PCR product was electrophoresed in 2% agarose gel, and was measured using ImageJ software (<http://rsb.info.nih.gov/ij/>) to calculate the ratio of each gene to *Gapdh*. The expression level for each gene is determined relative to that of *Gapdh*, and expression level in CL6 cells treated with DMSO alone was regarded as 1.0. The relative expression levels were averaged from at least three independent experiments.

Found at: doi:10.1371/journal.pone.0002407.s001 (1.04 MB DOC)

**Figure S2** Grem1 enhanced cardiomyogenic differentiation of mouse ES cells. Mouse ES cells (NCH1.5, C57BL/6j  $\times$  129ter/Sv) were cultured on a mouse embryonic fibroblast feeder layer inactivated with 30 Gy  $\gamma$ -irradiation in gelatin-coated 60 mm dishes (Becton, Dickinson). Cells were grown in KnockOut DMEM (Gibco) supplemented with 15% fetal bovine serum (Cell Culture Technologies), 2 mM GlutaMAX (Gibco), 0.1 mM non-essential amino acid (Gibco), 0.1 mM 2-mercaptoethanol (Gibco), penicillin, streptomycin, and 2,000 U/ml mouse leukemia inhibitory factor (LIF) (Chemicon). For cardiomyogenic differentiation, ES cells were exposed to 125 ng/ml Grem1 (R&D systems) for the three days. The cells were then trypsinized and cultured to form embryonic bodies (EBs) from a single cell using a three-dimensional culture system (without LIF) on low cell binding dishes (96-well plate round bottom). This represented day 0 of EB formation. On the next day, the medium was replaced with the same medium without LIF. EBs were re-seeded on gelatin-coated 48-well plates with one EB per well, on day 8 after the start of EB formation. The cardiomyogenic induction was estimated by the beating EB number per total EB number, measured on day 12 under a phase-contrast microscope. Grem1 increased the percentage of beating EBs to 69.2%, as compared with 26.7% in EBs without Grem1 treatment. The numbers in parentheses indicate the EB numbers counted.

Found at: doi:10.1371/journal.pone.0002407.s002 (1.27 MB DOC)

### Table S1 Primer sequences.

Found at: doi:10.1371/journal.pone.0002407.s003 (0.06 MB DOC)

**Movie S1** CL6 cells treated with DMSO alone. P19CL6 cells are reproducibly and stably induced into beating cardiomyocytes with DMSO.

Found at: doi:10.1371/journal.pone.0002407.s004 (1.66 MB MOV)

**Movie S2** CL6 cells treated with Grem1 (125 ng/ml) and DMSO. Grem1 dramatically promotes DMSO-induced cardiomyogenic differentiation of P19CL6 cells at a concentration of 125 ng/ml.

Found at: doi:10.1371/journal.pone.0002407.s005 (2.40 MB MOV)

## Acknowledgments

We would like to express our sincere thanks to T. Imamura and K. Miyazono for the *Id1* promoter-Lux plasmid, and J. Fujimoto for their discussion of this work.



## Author Contributions

Conceived and designed the experiments: AU DK. Performed the experiments: DK HM RI KM. Analyzed the data: AU AN DK YT RI

## References

- Andreec B, Duprez D, Vorbusch B, Arnold HH, Brand T (1998) BMP-2 induces ectopic expression of cardiac lineage markers and interferes with somite formation in chicken embryos. *Mech Dev* 70: 119–131.
- Schultheis TM, Burch JB, Lassar AB (1997) A role for bone morphogenetic proteins in the induction of cardiac myogenesis. *Genes Dev* 11: 451–462.
- Angello JC, Kaestner S, Welikson RE, Buskin JN, Hauschka SD (2006) BMP induction of cardiogenesis in P19 cells requires prior cell-cell interaction(s). *Dev Dyn* 235: 2122–2133.
- Asan BH, Schultheis TM (2002) Regulation of avian cardiogenesis by Fgf8 signaling. *Development* 129: 1935–1943.
- Crossley PH, Martin GR (1995) The mouse Fgf8 gene encodes a family of polypeptides and is expressed in regions that direct outgrowth and patterning in the developing embryo. *Development* 121: 439–451.
- Reifers F, Walsh EC, Leger S, Stainier DY, Brand M (2000) Induction and differentiation of the zebrafish heart requires fibroblast growth factor 8 (fgf8/acerebellar). *Development* 127: 225–235.
- Whitehead GG, Makino S, Lien CL, Keating MT (2005) fgf20 is essential for initiating zebrafish fin regeneration. *Science* 310: 1957–1960.
- Yamagishi H, Olson EN, Srivastava D (2000) The basic helix-loop-helix transcription factor, dHAND, is required for vascular development. *J Clin Invest* 105: 261–270.
- Arizumi T, Kishimoto M, Yokota C, Takano K, Fukuda K, et al. (2003) Amphibian in vitro heart induction: a simple and reliable model for the study of vertebrate cardiac development. *Int J Dev Biol* 47: 405–410.
- Gavert N, Ben-Ze'ev A (2007) beta-Catenin signaling in biological control and cancer. *J Cell Biochem* 102: 820–828.
- Chien KR, Moretti A, Laugwitz KL (2004) Development. ES cells to the rescue. *Science* 306: 239–240.
- Pandur P, Lasche M, Eisenberg LM, Kuhl M (2002) Wnt-11 activation of a non-canonical Wnt signalling pathway is required for cardiogenesis. *Nature* 418: 636–641.
- Yamagishi H, Yamagishi C, Nakagawa O, Harvey RP, Olson EN, et al. (2001) The combinatorial activities of Nkx2.5 and dHAND are essential for cardiac ventricle formation. *Dev Biol* 239: 190–203.
- Park M, Wu X, Golden K, Axelrod JD, Bodmer R (1996) The wingless signaling pathway is directly involved in Drosophila heart development. *Dev Biol* 177: 104–116.
- Marvin MJ, Di Rocco G, Gardiner A, Bush SM, Lassar AB (2001) Inhibition of Wnt activity induces heart formation from posterior mesoderm. *Genes Dev* 15: 316–327.
- Schneider VA, Mercola M (2001) Wnt antagonism initiates cardiogenesis in *Xenopus laevis*. *Genes Dev* 15: 304–315.
- Tzahor E, Lassar AB (2001) Wnt signals from the neural tube block ectopic cardiogenesis. *Genes Dev* 15: 255–260.
- Olson EN (2001) Development. The path to the heart and the road not taken. *Science* 291: 2327–2328.
- Terami H, Hidaka K, Katsumata T, Iio A, Morisaki T (2004) Wnt11 facilitates embryonic stem cell differentiation to Nkx2.5-positive cardiomyocytes. *Biochem Biophys Res Commun* 325: 968–975.
- Sharov AA, Dudekula DB, Ko MS (2005) A web-based tool for principal component and significance analysis of microarray data. *Bioinformatics* 21: 2548–2549.
- Hamatani T, Carter MG, Sharov AA, Ko MS (2004) Dynamics of global gene expression changes during mouse preimplantation development. *Dev Cell* 6: 117–131.
- Sharov AA, Dudekula DB, Ko MS (2005) <http://lguun.grc.nia.nih.gov/ANOVA/help.html#hierarchical> Accessed 2007 April 20. *Bioinformatics Advance Access*.
- Naito AT, Akazawa H, Takano H, Minamoto T, Nagai T, et al. (2005) Phosphatidylinositol 3-kinase-Akt pathway plays a critical role in early cardiomyogenesis by regulating canonical Wnt signaling. *Circ Res* 97: 144–151.
- Hsu DR, Economides AN, Wang X, Eimon PM, Harland RM (1998) The *Xenopus* dorsalizing factor Gremlin identifies a novel family of secreted proteins that antagonize BMP activities. *Mol Cell* 1: 673–683.
- Naito AT, Shiojima I, Akazawa H, Hidaka K, Morisaki T, et al. (2006) Developmental stage-specific biphasic roles of Wnt/beta-catenin signaling in cardiomyogenesis and hematopoiesis. *Proc Natl Acad Sci U S A* 103: 19812–19817.
- Jin EJ, Erickson CA, Takada S, Burrus LW (2001) Wnt and BMP signaling governs lineage segregation of melanocytes in the avian embryo. *Dev Biol* 233: 22–37.
- Sutherland MK, Geoghegan JC, Yu C, Turcott E, Skonier JE, et al. (2004) Sclerostin promotes the apoptosis of human osteoblastic cells: a novel regulation of bone formation. *Bone* 35: 828–835.
- Shi W, Zhao J, Anderson KD, Warburton D (2001) Gremlin negatively modulates BMP4 induction of embryonic mouse lung branching morphogenesis. *Am J Physiol Lung Cell Mol Physiol* 280: L1030–1039.
- Tzahor E, Kempf H, Mootosamy RC, Poon AC, Abzhanov A, et al. (2003) Antagonists of Wnt and BMP signaling promote the formation of vertebrate head muscle. *Genes Dev* 17: 3087–3099.
- Zuniga A, Michos O, Spitz F, Haramis AP, Panman L, et al. (2004) Mouse limb deformity mutations disrupt a global control region within the large regulatory landscape required for Gremlin expression. *Genes Dev* 18: 1533–1564.
- Michos O, Panman L, Vintersten K, Beier K, Zeller R, et al. (2004) Gremlin-mediated BMP antagonism induces the epithelial-mesenchymal feedback signaling controlling metanephric kidney and limb organogenesis. *Development* 131: 3401–3410.
- Yuasa S, Itabashi Y, Koshimizu U, Tanaka T, Sugimura K, et al. (2005) Transient inhibition of BMP signaling by Noggin induces cardiomyocyte differentiation of mouse embryonic stem cells. *Nat Biotechnol* 23: 607–611.
- Singh JP, Chaikin MA, Pledger WJ, Scher CD, Stiles CD (1983) Persistence of the mitogenic response to platelet-derived growth factor (competence) does not reflect a long-term interaction between the growth factor and the target cell. *J Cell Biol* 96: 1497–1502.
- Frank NY, Kho AT, Schatton T, Murphy GF, Molloy MJ, et al. (2006) Regulation of myogenic progenitor proliferation in human fetal skeletal muscle by BMP4 and its antagonist Gremlin. *J Cell Biol* 175: 99–110.
- Klaus A, Saga Y, Takekoto MM, Tzahor E, Birchmeier W (2007) Distinct roles of Wnt/beta-catenin and Bmp signaling during early cardiogenesis. *Proc Natl Acad Sci U S A* 104: 18531–18536.
- Yamaguchi TP, Takada S, Yoshikawa Y, Wu N, McMahon AP (1999) T (Brachyury) is a direct target of Wnt3a during paraxial mesoderm specification. *Genes Dev* 13: 3185–3190.
- Kleber M, Lee HY, Wurdak H, Buchstaller J, Riccomagno MM, et al. (2005) Neural crest stem cell maintenance by combinatorial Wnt and BMP signaling. *J Cell Biol* 169: 309–320.
- Sugiki T, Uyama T, Toyoda M, Morioka H, Kume S, et al. (2007) Hyaline cartilage formation and endochondral ossification modeled with KUM5 and OP9 chondroblasts. *J Cell Biochem* 100: 1240–1254.

MT MW. Contributed reagents/materials/analysis tools: IK AN IS HS. Wrote the paper: AU DK.

## IGFBP-4 is an inhibitor of canonical Wnt signalling required for cardiogenesis

Weidong Zhu<sup>1\*</sup>, Ichiro Shiojima<sup>1\*</sup>, Yuzuru Ito<sup>2\*</sup>, Zhi Li<sup>1</sup>, Hiroyuki Ikeda<sup>1</sup>, Masashi Yoshida<sup>1</sup>, Atsuhiko T. Naito<sup>1</sup>, Jun-ichiro Nishi<sup>1</sup>, Hiroo Ueno<sup>3</sup>, Akihiro Umezawa<sup>4</sup>, Tooru Minamino<sup>1</sup>, Toshio Nagai<sup>1</sup>, Akira Kikuchi<sup>3</sup>, Makoto Asashima<sup>2,6,7</sup> & Issei Komuro<sup>1</sup>

Insulin-like growth-factor-binding proteins (IGFBPs) bind to and modulate the actions of insulin-like growth factors (IGFs)<sup>1</sup>. Although some of the actions of IGFBPs have been reported to be independent of IGFs, the precise mechanisms of IGF-independent actions of IGFBPs are largely unknown<sup>1,2</sup>. Here we report a previously unknown function for IGFBP-4 as a cardiogenic growth factor. IGFBP-4 enhanced cardiomyocyte differentiation *in vitro*, and knockdown of *Igfbp4* attenuated cardiomyogenesis both *in vitro* and *in vivo*. The cardiogenic effect of IGFBP-4 was independent of its IGF-binding activity but was mediated by the inhibitory effect on canonical Wnt signalling. IGFBP-4 physically interacted with a Wnt receptor, Frizzled 8 (Frz8), and a Wnt co-receptor, low-density lipoprotein receptor-related protein 6 (LRP6), and inhibited the binding of Wnt3A to Frz8 and LRP6. Although IGF-independent, the cardiogenic effect of IGFBP-4 was attenuated by IGFs through IGFBP-4 sequestration. IGFBP-4 is therefore an inhibitor of the canonical Wnt signalling required for cardiogenesis and provides a molecular link between IGF signalling and Wnt signalling.

The heart is the first organ to form during embryogenesis, and abnormalities in this process result in congenital heart diseases, the most common cause of birth defects in humans<sup>3</sup>. Molecules that mediate cardiogenesis are of particular interest because of their potential use for cardiac regeneration<sup>4,5</sup>. Previous studies have shown that soluble growth factors such as bone morphogenetic proteins (BMPs), fibroblast growth factors (FGFs), Wnts and Wnt inhibitors mediate the tissue interactions that are crucial for cardiomyocyte specification<sup>3,4</sup>. We proposed that there might be additional soluble factors that modulate cardiac development and/or cardiomyocyte differentiation.

P19CL6 cells differentiate into cardiomyocytes with high efficiency in the presence of 1% dimethylsulphoxide (DMSO)<sup>6</sup>. We cultured P19CL6 cells with culture media conditioned by various cell types in the absence of DMSO, and screened the cardiogenic activity of the conditioned media. The extent of cardiomyocyte differentiation was assessed by the immunostaining with MF20 monoclonal antibody that recognizes sarcomeric myosin heavy chain (MHC). Among the several cell types tested, culture media conditioned by a murine stromal cell line OP9 induced cardiomyocyte differentiation of P19CL6 cells without DMSO treatment (Fig. 1a, left and middle panels). Increased MF20-positive area was accompanied by the induction of cardiac marker genes such as  $\alpha$ MHC, *Nkx2.5* and *GATA-4*, and by the increased protein levels of cardiac troponin T (cTnT) (Fig. 1a,

right panel). In contrast, culture media conditioned by COS7 cells, mouse embryonic fibroblasts, NIH3T3 cells, HeLa cells, END2 cells (visceral endoderm-like cells), neonatal rat cardiomyocytes and neonatal rat cardiac fibroblasts did not induce cardiomyocyte differentiation of P19CL6 cells in the absence of DMSO (Fig. 1a and data not shown). From these observations, we postulated that OP9 cells secrete one or more cardiogenic growth factors.

To identify an OP9-derived cardiogenic factor, complementary DNA clones isolated by a signal sequence trap method from an OP9 cell cDNA library<sup>7</sup> were tested for their cardiogenic activities by transient transfection. When available, recombinant proteins were also used to confirm the results. Among candidate factors tested, IGFBP-4 induced cardiomyocyte differentiation of P19CL6 cells, as demonstrated by the increase in MF20-positive area and the induction of cardiac markers (Fig. 1b). We also cultured P19CL6 cells with OP9-conditioned media pretreated with an anti-IGFBP-4 neutralizing antibody. The application of an anti-IGFBP-4 neutralizing antibody attenuated the efficiency of cardiomyocyte differentiation induced by OP9-conditioned media (Fig. 1c). These findings strongly suggest that IGFBP-4 is a cardiogenic factor secreted from OP9 cells.

Because IGFBPs have been characterized as molecules that bind to and modulate the actions of IGFs, we tested whether IGFBP-4 promotes cardiogenesis by either enhancing or inhibiting the actions of IGFs. We first treated P19CL6 cells with a combination of anti-IGF-I and IGF-II-neutralizing antibodies or a neutralizing antibody against type-I IGF receptor. If IGFBP-4 induces cardiomyocyte differentiation by inhibiting IGF signalling, treatment with these antibodies should induce cardiomyocyte differentiation and/or enhance the cardiogenic effects of IGFBP-4. In contrast, if IGFBP-4 promotes cardiogenesis by enhancing IGF signalling, treatment with these antibodies should attenuate IGFBP-4-mediated cardiogenesis. However, treatment with these antibodies did not affect the efficiency of IGFBP-4-induced cardiomyocyte differentiation (Fig. 1d and data not shown). Treatment of P19CL6 cells with IGF-I and IGF-II also did not induce cardiomyocyte differentiation (data not shown). Furthermore, treatment with an IGFBP-4 mutant (IGFBP-4-H74P; His74 replaced by Pro)<sup>8</sup> that is unable to bind IGFs induced cardiomyocyte differentiation of P19CL6 cells even more efficiently than wild-type IGFBP-4 (Fig. 1e). This is presumably due to the sequestration of wild-type IGFBP-4 but not mutant IGFBP-4-H74P by endogenous IGFs. In agreement with this idea, exogenous IGFs attenuated wild-type IGFBP-4-induced but not IGFBP-4-H74P-induced cardiogenesis (Fig. 1f). Taken together, these observations indicate

<sup>1</sup>Department of Cardiovascular Science and Medicine, Chiba University Graduate School of Medicine, Chiba 260-8670, Japan. <sup>2</sup>CORP Organ Regeneration Project, Japan Science and Technology Agency (JST), Tokyo 153-8902, Japan. <sup>3</sup>Institute of Stem Cell Biology and Regenerative Medicine, Stanford University School of Medicine, Stanford, California 94305, USA. <sup>4</sup>Department of Reproductive Biology, National Institute for Child Health and Development, Tokyo 157-8535, Japan. <sup>5</sup>Department of Biochemistry, Graduate School of Biomedical Sciences, Hiroshima University, Hiroshima 734-8551, Japan. <sup>6</sup>Department of Life Sciences (Biology), Graduate School of Arts and Science, The University of Tokyo, Tokyo 153-8902, Japan. <sup>7</sup>National Institute of Advanced Industrial Sciences and Technology (AIST), Ibaraki 305-8562, Japan.

\*These authors contributed equally to this work.



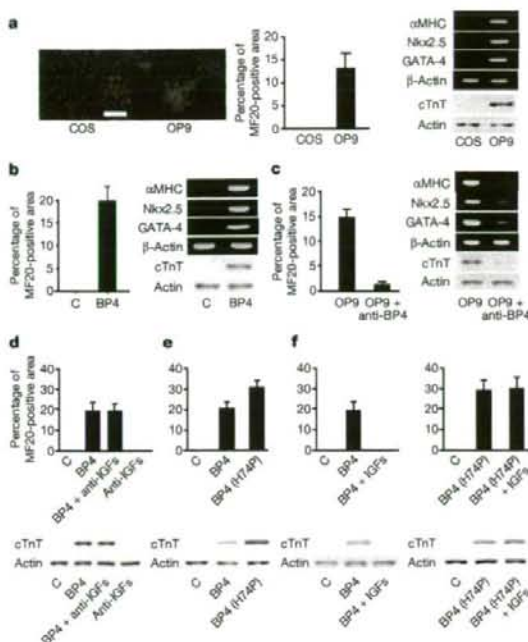


**Figure 1 | IGFBP-4 promotes cardiomyocyte differentiation in an IGF-independent manner.** **a**, Culture media conditioned by OP9 cells but not by COS7 cells induced cardiomyocyte differentiation of P19CL6 cells as assessed by MF20-positive area, cardiac marker-gene expression and cTnT protein expression. Scale bar, 100 μm. Error bars show s.d. **b**, Treatment with IGFBP-4 (1 μg ml<sup>-1</sup>) induced cardiomyocyte differentiation of P19CL6 cells in the absence of DMSO. Error bars show s.d. **c**, Treatment with a neutralizing antibody against IGFBP-4 (anti-BP4; 40 μg ml<sup>-1</sup>) attenuated cardiomyocyte differentiation of P19CL6 cells induced by OP9-conditioned media. Error bars show s.d. **d**, Treatment with neutralizing antibodies against IGF-I and IGF-II (anti-IGFs; 5 μg ml<sup>-1</sup> each) had no effect on IGFBP-4-induced cardiomyocyte differentiation of P19CL6 cells. Error bars show s.d. **e**, Mutant IGFBP-4 (BP4(H74P)) that is incapable of binding to IGFs retained cardiomyogenic activity. Error bars show s.d. **f**, IGFs (100 ng ml<sup>-1</sup> each) attenuated wild-type IGFBP-4-induced but not mutant IGFBP-4-H74P-induced cardiomyocyte differentiation of P19CL6 cells. Error bars show s.d.

that IGFBP-4 induces cardiomyocyte differentiation in an IGF-independent fashion.

To explore further the mechanisms by which IGFBP-4 induces cardiomyogenesis, we tested the hypothesis that IGFBP-4 might modulate the signals activated by other secreted factors implicated in cardiogenesis. It has been shown that canonical Wnt signalling is crucial in cardiomyocyte differentiation<sup>34</sup>. In P19CL6 cells, Wnt3A treatment activated β-catenin-dependent transcription of the TOPFLASH reporter gene, and this activation was attenuated by IGFBP-4 (Fig. 2a). Wnt/β-catenin signalling is transduced by the cell-surface receptor complex consisting of Frizzled and low-density-lipoprotein receptor (LDLR)-related protein 5/6 (LRP5/6)<sup>9</sup> and IGFBP-4 attenuated TOPFLASH activity enhanced by the expression of LRP6 or Frizzled 8 (Frz8) (Fig. 2a). As a control, IGFBP-4 did not alter BMP-mediated activation of a BMP-responsive reporter BRE-luc (Supplementary Fig. 1b). These findings suggest that IGFBP-4 is a specific inhibitor *in vivo* of the canonical Wnt pathway. To examine this possibility *in vivo*, we performed axis duplication assays in *Xenopus* embryos. Injection of *Xwnt8* or *Lrp6* mRNA caused secondary axis formation, and injection of *Xenopus IGFBP-4* (*XIGFBP-4*) mRNA alone had minimal effects on axis

formation. However, *Xwnt8*-induced or LRP6-induced secondary axis formation was efficiently blocked by coexpression of *XIGFBP-4* (Fig. 2b, c), indicating that IGFBP-4 inhibits canonical Wnt signalling *in vivo*. To explore the mechanisms of Wnt inhibition by IGFBP-4, *Xenopus* animal cap assays and TOPFLASH reporter gene assays were performed. In animal cap assays, IGFBP-4 inhibited LRP6-induced but not β-catenin-induced Wnt-target gene expression (Supplementary Fig. 1c). Similarly, IGFBP-4 attenuated Wnt3A-induced or LRP6-induced TOPFLASH activity but did not alter Dishevelled-1 (Dvl-1)-induced, LiCl-induced or β-catenin-induced TOPFLASH activity (Supplementary Fig. 1d, e). These findings suggest that IGFBP-4 inhibits canonical Wnt signalling at the level of cell-surface receptors. To examine whether IGFBP-4 antagonizes Wnt signalling via direct physical interaction with LRP5/6 or Frizzled, we produced conditioned media containing the Myc-tagged extracellular portion of LRP6 (LRP6N-Myc), the Myc-tagged cysteine-rich domain (CRD) of Frz8 (Frz8CRD-Myc), and V5-tagged IGFBP-4 (IGFBP-4-V5). Immunoprecipitation (IP)/western blot experiments revealed that IGFBP-4 interacted with LRP6N (Fig. 2d) and Frz8CRD (Fig. 2e). A liquid-phase binding assay with <sup>125</sup>I-labelled IGFBP-4 and conditioned media containing LRP6N-Myc or Frz8CRD-Myc demonstrated that the interaction between IGFBP-4 and LRP6N or Frz8CRD was specific and saturable (Fig. 2f, g). A Scatchard plot analysis revealed two binding sites with different binding affinities for LRP6N (Fig. 2f, inset) and a single binding site for Frz8CRD (Fig. 2g, inset). A similar binding assay with <sup>125</sup>I-labelled Wnt3A demonstrated that IGFBP-4 inhibited Wnt3A binding to LRP6N (Fig. 2h) and Frz8CRD (Fig. 2i), and a Lineweaver-Burk plot revealed that IGFBP-4 was a competitive inhibitor of the binding of Wnt3A to Frz8CRD (Supplementary Fig. 2a). IP/western blot analysis with various deletion mutants of LRP6 and IGFBP-4 revealed that IGFBP-4 interacted with multiple domains of LRP6 and that the carboxy-terminal thyroglobulin domain of IGFBP-4 was required for IGFBP-4 binding to LRP6 or Frz8CRD (Supplementary Fig. 2b–f). It has been shown that inhibition of canonical Wnt signalling promotes cardiomyocyte differentiation in embryonic stem (ES) cells and in chick, *Xenopus* and zebrafish embryos<sup>41,42</sup>. These results therefore collectively suggest that IGFBP-4 promotes cardiogenesis by antagonizing the Wnt/β-catenin pathway through direct interactions with Frizzled and LRP5/6.

Next we investigated the role of endogenous IGFBP-4 in P19CL6 cell differentiation into cardiomyocytes. Reverse transcriptase-mediated polymerase chain reaction (RT-PCR) analysis revealed that the expression of *Igfbp4* was upregulated during DMSO-induced P19CL6 cell differentiation (Fig. 3a). Expression of *Igfbp3* and *Igfbp5* was also upregulated in the early and the late phases of differentiation, respectively. Expression of *Igfbp2* was not altered, and that of *Igfbp1* or *Igfbp6* was not detected. When IGFBP-4 was knocked down by two different small interfering RNA (siRNA) constructs, DMSO-induced cardiomyocyte differentiation was inhibited in both cases (Fig. 3b). In contrast, knockdown of *Igfbp3* or *Igfbp5* did not inhibit DMSO-induced cardiomyocyte differentiation (Fig. 3b, right panel). Treatment with an anti-IGFBP-4 neutralizing antibody also blocked DMSO-induced cardiomyocyte differentiation (Fig. 3c). Secretion of endogenous IGFBP-4 is therefore required for the differentiation of P19CL6 cells into cardiomyocytes. Immunostaining for IGFBP-4 revealed that cardiac myocytes were surrounded by the IGFBP-4-positive cells, suggesting that a paracrine effect of IGFBP-4 on cardiomyocyte differentiation is predominant (Fig. 3d). Essentially the same results were obtained in ES cells (Supplementary Fig. 3d–g). To investigate whether IGFBP-4 promotes the differentiation of P19CL6 cells into cardiomyocytes by the inhibition of the canonical Wnt pathway, we expressed dominant-negative LRP6 (LRP6N) in P19CL6 cells. Expression of LRP6N enhanced cardiomyocyte differentiation of P19CL6 cells and reversed the inhibitory effect of *Igfbp4*

knockdown on cardiomyogenesis (Fig. 3e). These observations suggest that endogenous IGFBP-4 is required for cardiomyocyte differentiation of P19CL6 cells and ES cells, and that the cardiogenic effect of IGFBP-4 is mediated by its inhibitory effect on Wnt/ $\beta$ -catenin signalling.

The role of endogenous IGFBP-4 in cardiac development *in vivo* was also examined with *Xenopus* embryos. Whole-mount *in situ* hybridization analysis revealed that strong expression of *XIGFBP-4* was detected at stage 38 in the anterior part of the liver adjacent to the heart (Fig. 4a). Knockdown of *XIGFBP-4* by two different morpholino (MO) constructs resulted in cardiac defects, with more than 70% of the embryos having a small heart or no heart (Fig. 4b). The specificity of MO was confirmed by the observation that simultaneous injection of MO-resistant *XIGFBP-4* cDNA rescued the MO-induced cardiac defects (Fig. 4b, Supplementary Fig. 4c). Coexpression of IGF-binding-defective *XIGFBP-4* mutant (*XIGFBP-4*-H74P) or

dominant-negative LRP6 (LRP6N) also rescued the cardiac defects induced by *XIGFBP-4* knockdown (Fig. 4b), whereas overexpression of *Xwnt8* in the heart-forming region resulted in cardiac defects similar to those induced by *XIGFBP-4* knockdown (Supplementary Fig. 4d–f), supporting the notion that the cardiogenic effect of IGFBP-4 is independent of IGFs but is mediated by inhibition of the Wnt/ $\beta$ -catenin pathway. The temporal profile of cardiac defects induced by *XIGFBP-4* knockdown was also examined by *in situ* hybridization with *cardiac troponin I* (*cTnl*) (Fig. 4c). At stage 34, morphology of the heart was comparable between control embryos and MO-injected embryos. However, at stage 38, when *XIGFBP-4* starts to be expressed in the anterior part of the liver, the expression of *cTnl* was markedly attenuated in MO-injected embryos; expression of *cTnl* was diminished and no heart-like structure was observed at stage 42. Thus, the heart is initially formed but its subsequent growth is perturbed in the absence of IGFBP-4, suggesting that IGFBP-4

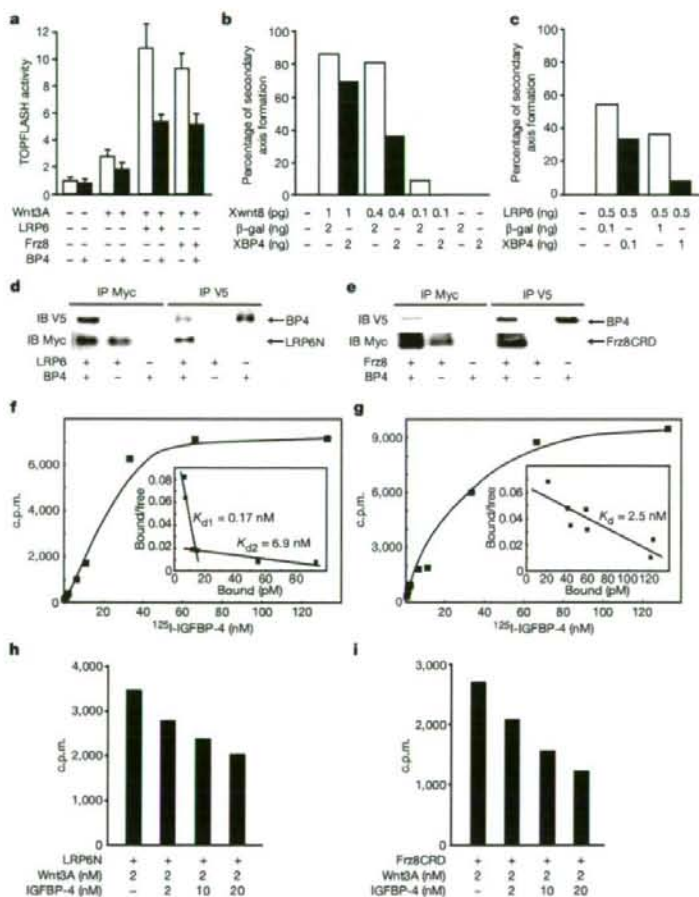


**Figure 2** | IGFBP-4 inhibits Wnt/ $\beta$ -catenin signalling through direct interactions with Wnt receptors. **a**, IGFBP-4 attenuated  $\beta$ -catenin-independent transcription in P19CL6 cells. P19CL6 cells were transfected with TOPFLASH reporter gene and expression vectors for LRP6 or Frz8, and then treated with Wnt3A or Wnt3A plus IGFBP-4; luciferase activities were then measured. Error bars show s.d. **b**, IGFBP-4 (XBP4) inhibited Xwnt8-induced secondary-axis formation in *Xenopus* embryos ( $n = 20$  for each group). **c**, IGFBP-4 inhibited LRP6-induced secondary-axis formation in *Xenopus* embryos ( $n = 30$  for each group). **d**, **e**, IGFBP-4 interacted directly

with LRP6N (**d**) and Frz8CRD (**e**). IB, immunoblotting; IP, immunoprecipitation. **f**, A binding assay between  $^{125}$ I-labelled IGFBP-4 and LRP6N. The inset is a Scatchard plot showing two binding sites with different binding affinities. **g**, A binding assay between  $^{125}$ I-labelled IGFBP-4 and Frz8CRD. The inset is a Scatchard plot showing a single binding site. **h**, **i**, IGFBP-4 inhibited Wnt3A binding to LRP6N (**h**) or Frz8CRD (**i**).  $^{125}$ I-labelled Wnt3A binding to LRP6N or Frz8CRD was assessed in the presence of increasing amounts of IGFBP-4.



promotes cardiogenesis by maintaining the proliferation and/or survival of embryonic cardiomyocytes.

It has been shown that canonical Wnt signals inhibit cardiogenesis in chick and frog embryos, and that Wnt antagonists such as Dkk1 and Crescent secreted from the anterior endoderm or the organizer region counteract the Wnt-mediated inhibitory signals and induce cardiogenesis in the anterior lateral mesoderm<sup>1</sup>. However, IGFBP-4-mediated Wnt inhibition is required at later stages of development, when the heart is already formed at the ventral portion and starts to grow and remodel to maintain embryonic circulation. It has been shown that Wnt/ $\beta$ -catenin signalling has time-dependent effects on cardiogenesis in ES cells: canonical Wnt signalling in the early phase of ES-cell differentiation promotes cardiomyogenesis, whereas it inhibits cardiomyocyte differentiation in the late phase<sup>10–12</sup>. In agreement with this notion, IGFBP-4 promoted cardiomyocyte differentiation of ES cells only when IGFBP-4 was applied in the late phase after embryoid body formation (Supplementary Fig. 3a–c). Similar

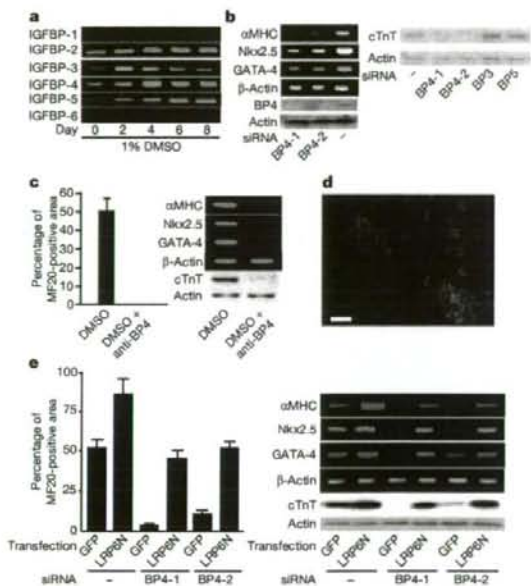


**Figure 3 | IGFBP-4 is required for the differentiation of P19CL6 cells into cardiomyocytes.** **a**, Expression analysis of IGFBP family members by RT-PCR during DMSO-induced cardiomyocyte differentiation of P19CL6 cells (from day 0 to day 8). **b**, Left: knockdown of *Igfbp4* in P19CL6 cells attenuated cardiac marker expression in response to treatment with DMSO. BP4-1 and BP4-2 represent two different siRNAs for IGFBP-4. Right: knockdown of *Igfbp3* or *Igfbp5* had no effect on cTnT expression in response to DMSO treatment. **c**, Treatment with a neutralizing antibody against IGFBP-4 (anti-BP4; 40  $\mu$ g ml<sup>-1</sup>) attenuated DMSO-induced cardiomyocyte differentiation of P19CL6 cells. Error bars show s.d. **d**, IGFBP-4 immunostaining during DMSO-induced differentiation of P19CL6 cells stably transfected with  $\alpha$ MHC-green fluorescent protein (GFP) reporter gene. Top left, IGFBP-4 staining (red); top right, GFP expression representing differentiated cardiomyocytes; bottom left, nuclear staining with DAPI (4',6-diamidino-2-phenylindole); bottom right, a merged picture. Scale bar, 100  $\mu$ m. **e**, Attenuated cardiomyocyte differentiation of P19CL6 cells by *Igfbp4* knockdown was rescued by inhibiting Wnt/ $\beta$ -catenin signalling. Control and *Igfbp4*-knocked-down P19CL6 cells were transfected with an expression vector for GFP or LRP6N (a dominant-negative form of LRP6) and induced to differentiate into cardiomyocytes by treatment with DMSO. LRP6N overexpression rescued the attenuated cardiomyocyte differentiation induced by *Igfbp4* knockdown as assessed by MF20-positive area (left panel), cardiac marker-gene expression and cTnT protein expression (right panel). Error bars show s.d.

time-dependent effects of Wnt/ $\beta$ -catenin signalling on cardiogenesis has been shown in zebrafish embryos<sup>11</sup>. Moreover, several recent reports suggest that Wnt/ $\beta$ -catenin signalling is a positive regulator of cardiac progenitor-cell proliferation in the secondary heart field<sup>13</sup>. It therefore seems that canonical Wnt signalling has divergent effects on cardiogenesis at multiple stages of development: first, canonical Wnt signalling promotes cardiogenesis at the time of gastrulation or mesoderm specification; second, it inhibits cardiogenesis at the time when cardiac mesoderm is specified in the anterior lateral mesoderm; third, it promotes the expansion of cardiac progenitors in the secondary heart field; and fourth, it inhibits cardiogenesis at later stages when the embryonic heart is growing. It is interesting to note that IGFBP-4 is expressed predominantly in the liver. Mouse IGFBP-4 is

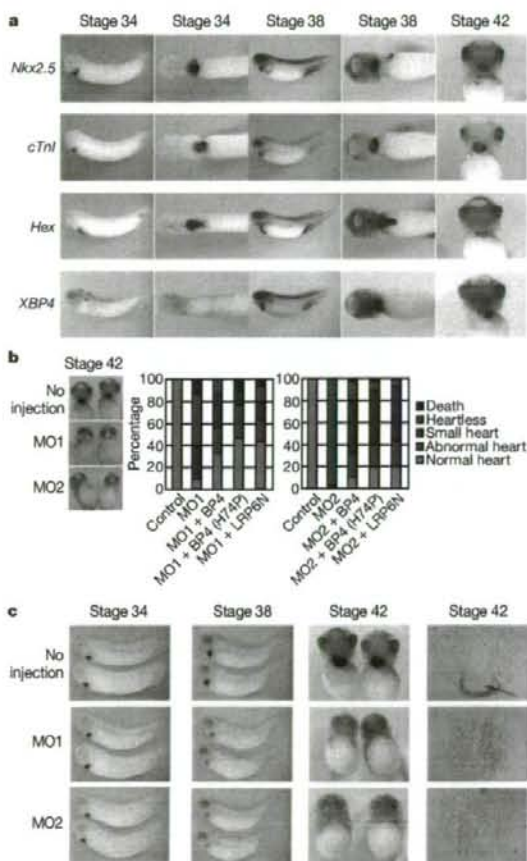


**Figure 4 | IGFBP-4 is required for the maturation of the heart in *Xenopus* embryos.** **a**, *In situ* hybridization analysis of *Nkx2.5* (an early cardiac marker), *cTnI* (a mature cardiac marker), *Hex* (a liver marker), and *XIGFBP-4* (*XBP4*) mRNA expression at stages 34, 38 and 42. **b**, Knockdown of *XIGFBP-4* by two different morpholinos (MO1 and MO2) resulted in severe cardiac defects as assessed by *cTnI* *in situ* hybridization at stage 42 (left). These cardiac defects were rescued by simultaneous injection of MO-resistant wild-type *XIGFBP-4*, mutant *XIGFBP-4*-H74P (BP4(H74P)) and LRP6N ( $n = 30$  for each group). **c**, Temporal profile of cardiac defects induced by *XIGFBP-4* knockdown. Morphology of the heart as assessed by *cTnI* *in situ* hybridization was almost normal at stage 34 but was severely perturbed at stages 38 and 42. The right column shows sections of control and MO-injected embryos. The arrow indicates the heart in control embryos. No heart-like structure was observed in MO-injected embryos.

also strongly expressed in the tissues adjacent to the heart such as pharyngeal arches and liver bud at embryonic day (E)9.5 (Supplementary Fig. 3h). These observations and the results of IGFBP-4 immunostaining in P19CL6 cells and ES cells suggest that IGFBP-4 promotes cardiogenesis in a paracrine fashion. Together with a previous report showing that cardiac mesoderm secretes FGFs and induces liver progenitors in the ventral endoderm<sup>14</sup>, these observations suggest that there exist reciprocal paracrine signals between the heart and the liver that coordinately promote the development of each other.

IGFBPs are composed of six members, IGFBP-1 to IGFBP-6. Reporter gene assays and  $\beta$ -catenin stabilization assays revealed that IGFBP-4 was the most potent canonical Wnt inhibitor and that IGFBP-1, IGFBP-2 and IGFBP-6 also showed modest activity in Wnt inhibition, whereas IGFBP-3 and IGFBP-5 had no such activity (Supplementary Fig. 5a–c). In agreement with this, IP/western blot analyses demonstrated that IGFBP-1, IGFBP-2, IGFBP-4 and IGFBP-6 but not IGFBP-3 or IGFBP-5 interacted with LRP6 or Frz8CRD (Supplementary Fig. 5d, e). Thus, the lack of cardiac phenotypes in IGFBP-4-null mice or IGFBP-3/IGFBP-4/IGFBP-5 triple knockout mice<sup>15</sup> may be due to genetic redundancies between IGFBP-4 and other IGFBPs such as IGFBP-1, IGFBP-2 and/or IGFBP-6.

The identification of IGFBP-4 as an inhibitor of Wnt/ $\beta$ -catenin signalling may also have some implications for cancer biology<sup>16</sup>. It was shown that treatment with IGFBP-4 reduces cell proliferation in some cancer cell lines *in vitro*, and that overexpression of IGFBP-4 attenuates the growth of prostate cancer *in vivo*. Decreased serum levels of IGFBP-4 are associated with the risk of breast cancer. Because the activation of Wnt signalling is implicated in several forms of malignant tumours<sup>17,18</sup>, it is possible that the inhibitory effect of IGFBP-4 on cell proliferation is mediated in part by the inhibition of canonical Wnt signalling.

#### METHODS SUMMARY

**Cell culture.** P19CL6 cells and ES cells were cultured and induced to differentiate into cardiomyocytes essentially as described<sup>19</sup>. P19CL6 cells (2,000 cells per 35-mm dish) were treated with various conditioned media for screening of their cardiogenic activities. For siRNA-mediated knockdown, pSIREN-RetroQ vectors (Clontech) ligated with double-stranded oligonucleotides were transfected into P19CL6 cells or ES cells, and puromycin-resistant clones were selected. **IP/western blot analyses and binding assays.** Conditioned media for IP/western blot analyses were produced by using 293 cells. Binding reactions were performed overnight at 4 °C. <sup>125</sup>I-labelling of IGFBP-4 and Wnt3A was performed with IODO-BEADS Iodination Reagent (Pierce). A liquid-phase binding assay was performed essentially as described<sup>19</sup>.

**Xenopus experiments.** Axis duplication assays, animal cap assays, and *in situ* hybridization analyses in *Xenopus* were performed essentially as described<sup>20</sup>. Electroporation of mRNA was performed at stage 28 essentially as described<sup>21</sup>.

**Full Methods** and any associated references are available in the online version of the paper at [www.nature.com/nature](http://www.nature.com/nature).

Received 22 August 2007; accepted 24 April 2008.

Published online 4 June 2008.

1. Firth, S. M. & Baxter, R. C. Cellular actions of the insulin-like growth factor binding proteins. *Endocr. Rev.* 23, 824–854 (2002).
2. Mohan, S. & Baylink, D. J. IGF-binding proteins are multifunctional and act via IGF-dependent and -independent mechanisms. *J. Endocrinol.* 175, 19–31 (2002).

3. Olson, E. N. & Schneider, M. D. Sizing up the heart: development redux in disease. *Genes Dev.* 17, 1937–1956 (2003).
4. Foley, A. & Mercola, M. Heart induction: embryology to cardiomyocyte regeneration. *Trends Cardiovasc. Med.* 14, 121–125 (2004).
5. Leri, A., Kajstura, J. & Anversa, P. Cardiac stem cells and mechanisms of myocardial regeneration. *Physiol. Rev.* 85, 1373–1416 (2005).
6. Monzen, K. et al. Bone morphogenetic proteins induce cardiomyocyte differentiation through the mitogen-activated protein kinase kinase TAK1 and cardiac transcription factors Csx/Nkx-2.5 and GATA-4. *Mol. Cell. Biol.* 19, 7096–7105 (1999).
7. Ueno, H. et al. A stromal cell-derived membrane protein that supports hematopoietic stem cells. *Nature Immunol.* 4, 457–463 (2003).
8. Qin, X., Strong, D. D., Baylink, D. J. & Mohan, S. Structure–function analysis of the human insulin-like growth factor binding protein-4. *J. Biol. Chem.* 273, 23509–23516 (1998).
9. Moon, R. T., Kohn, A. D., De Ferrari, G. V. & Kaykas, A. WNT and  $\beta$ -catenin signalling: diseases and therapies. *Nature Rev. Genet.* 5, 691–701 (2004).
10. Naito, A. T. et al. Developmental stage-specific biphasic roles of Wnt/ $\beta$ -catenin signaling in cardiomyogenesis and hematopoiesis. *Proc. Natl Acad. Sci. USA* 103, 19812–19817 (2006).
11. Ueno, S. et al. Biphasic role for Wnt/ $\beta$ -catenin signaling in cardiac specification in zebrafish and embryonic stem cells. *Proc. Natl Acad. Sci. USA* 104, 9685–9690 (2007).
12. Liu, Y. et al. Sox17 is essential for the specification of cardiac mesoderm in embryonic stem cells. *Proc. Natl Acad. Sci. USA* 104, 3859–3864 (2007).
13. Cohen, E. D., Tian, Y. & Morrissy, E. E. Wnt signaling: an essential regulator of cardiovascular differentiation, morphogenesis and progenitor self-renewal. *Development* 135, 789–798 (2008).
14. Jung, J., Zheng, M., Goldfarb, M. & Zaret, K. S. Initiation of mammalian liver development from endoderm by fibroblast growth factors. *Science* 284, 1998–2003 (1999).
15. Ning, Y. et al. Diminished growth and enhanced glucose metabolism in triple knockout mice containing mutations of insulin-like growth factor binding protein-3, -4, and -5. *Mol. Endocrinol.* 20, 2173–2186 (2006).
16. Durai, R. et al. Biology of insulin-like growth factor binding protein-4 and its role in cancer. *Int. J. Oncol.* 28, 1317–1325 (2006).
17. Logan, C. Y. & Nusse, R. The Wnt signaling pathway in development and disease. *Annu. Rev. Cell Dev. Biol.* 20, 781–810 (2004).
18. Clevers, H. Wnt/ $\beta$ -catenin signaling in development and disease. *Cell* 127, 469–480 (2006).
19. Semenov, M. V. et al. Head inducer Dickkopf-1 is a ligand for Wnt coreceptor LRP6. *Curr. Biol.* 11, 951–961 (2001).
20. Kobayashi, H. et al. Novel Daple-like protein positively regulates both the Wnt/ $\beta$ -catenin pathway and the Wnt/JNK pathway in *Xenopus*. *Mech. Dev.* 122, 1138–1153 (2005).
21. Sasagawa, S., Takabatake, T., Takabatake, Y., Muramatsu, T. & Takeshima, K. Improved mRNA electroporation method for *Xenopus* neurula embryos. *Genesis* 33, 81–85 (2002).

**Supplementary Information** is linked to the online version of the paper at [www.nature.com/nature](http://www.nature.com/nature).

**Acknowledgements** We thank E. Fujita, R. Kobayashi and Y. Ishiyama for technical support; T. Yamauchi and K. Ueki for advice on binding assays; and Y. Onuma and S. Takahashi for advice on *Xenopus* electroporation. This work was supported by grants from the Ministry of Education, Culture, Sports, Science and Technology (MEXT), the Ministry of Health, Labour, and Welfare, and the New Energy and Industrial Technology Development Organization (NEDO).

**Author Contributions** W.Z., I.S. and Y.I. contributed equally to this work. I.K. designed and supervised the research. W.Z., I.S., Y.I., Z.L., H.J., M.Y. and A.T.N. performed experiments. J.N., H.U., A.U., T.M., T.N., A.K. and M.A. contributed new reagents and/or analytical tools. W.Z., I.S., Y.I., A.K. and I.K. analysed data. W.Z., I.S., Y.I. and I.K. prepared the manuscript.

**Author Information** Reprints and permissions information is available at [www.nature.com/reprints](http://www.nature.com/reprints). Correspondence and requests for materials should be addressed to I.K. (komuro-ky@umin.ac.jp).